

Electronic Supplementary Information (ESI) for:

Electron-Accepting π-Conjugated Species with 1,8-Naphthalic Anhydride or Diketophosphanyl Units

Sergio Sánchez,^a Alva Yuen Yiu Woo,^a and Thomas Baumgartner^{ab*}

^a*Department of Chemistry, Centre for Advanced Solar Materials, University of Calgary, 2500 University Drive NW, Calgary, AB, T2N 1N4, Canada.*

^b*Department of Chemistry, York University, 4700 Keele Street, Toronto, ON, M3J 1P3, Canada.*

E-mail: tbaumgar@yorku.ca

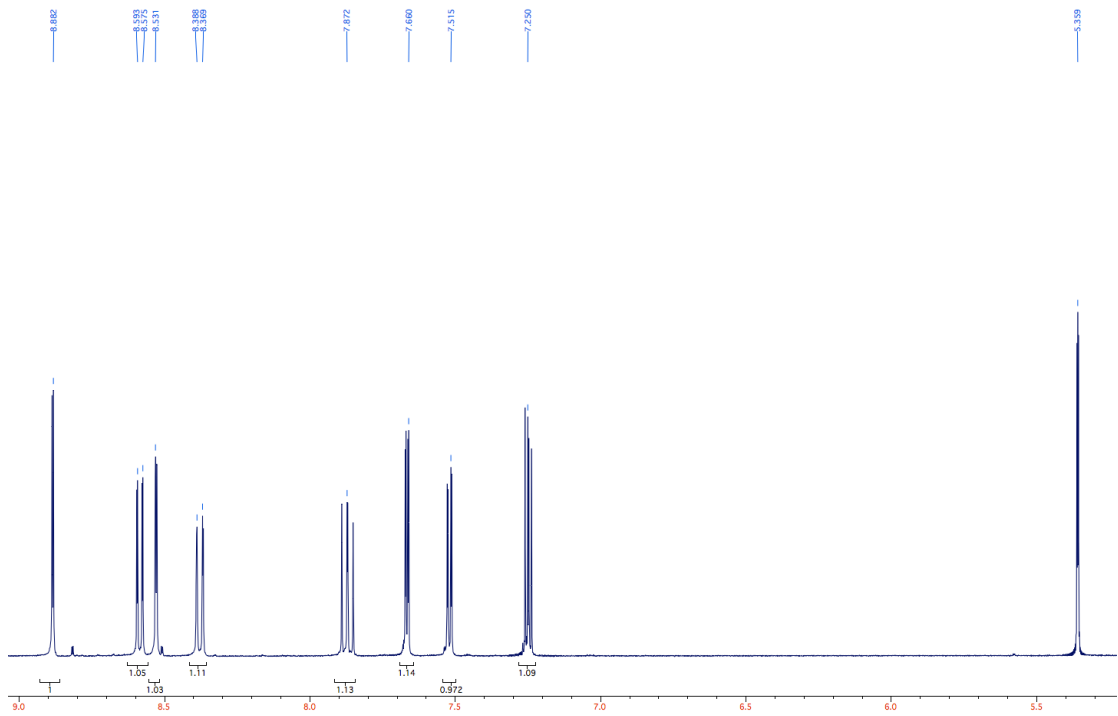


Figure S1: ^1H NMR spectrum of **2** in CD_2Cl_2 . Note: the inseparable impurities at 8.8 ppm and 8.55 ppm are from the Br-substituted anhydride starting material.

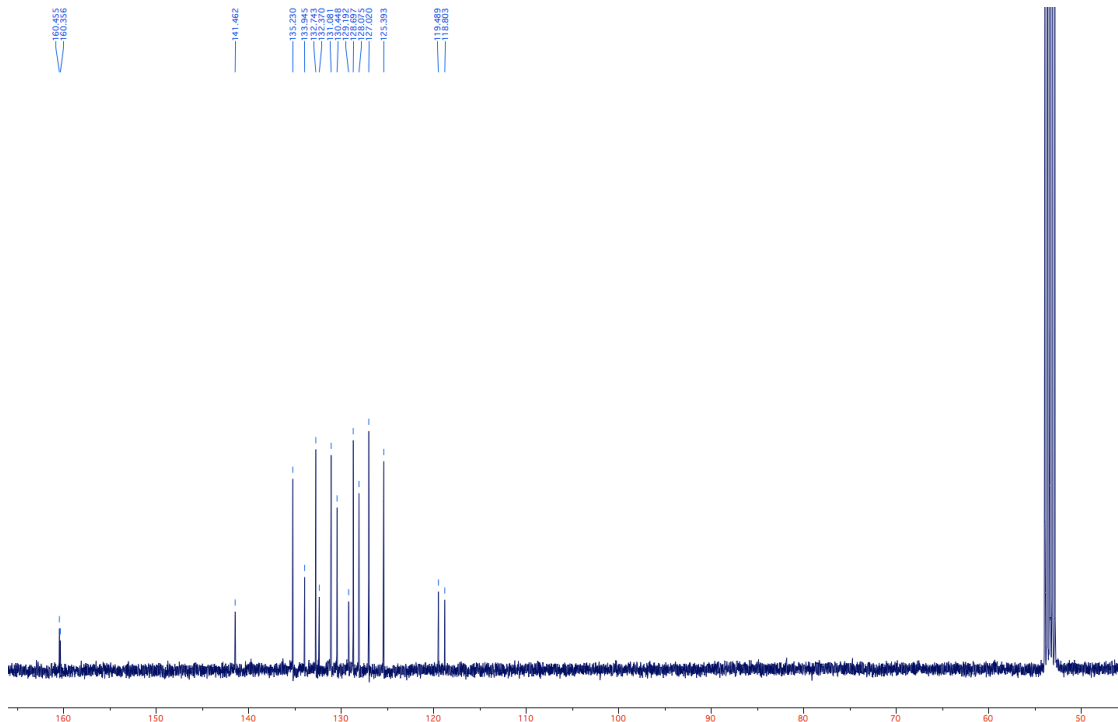


Figure S2: $^{13}\text{C}\{^1\text{H}\}$ NMR spectrum of **2** in CD_2Cl_2 .

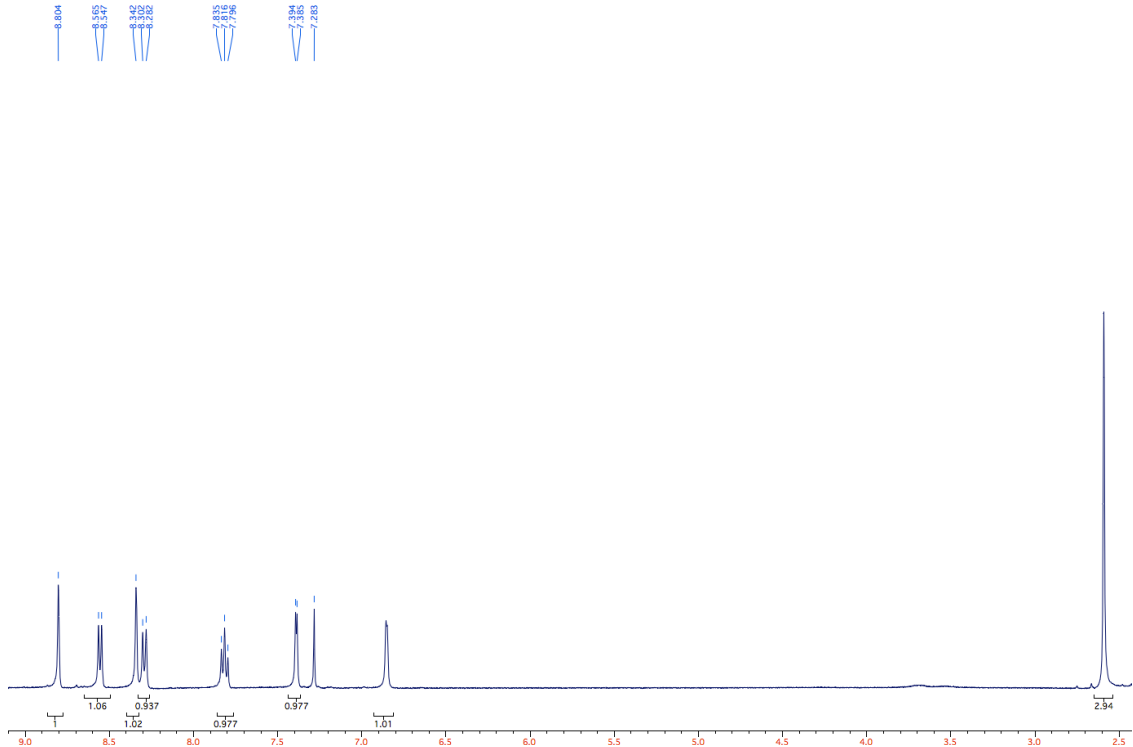


Figure S3: ^1H NMR spectrum of **3** in CD_2Cl_2 .

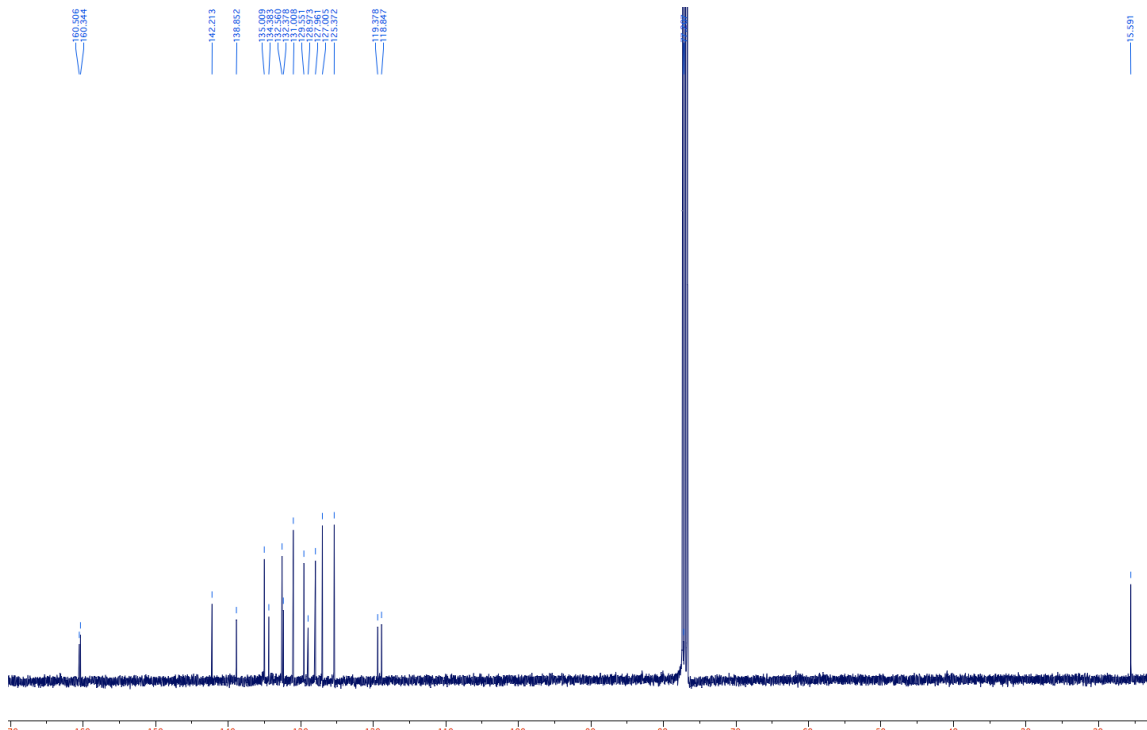


Figure S4: $^{13}\text{C}\{^1\text{H}\}$ NMR spectrum of **3** in CD_2Cl_2 .

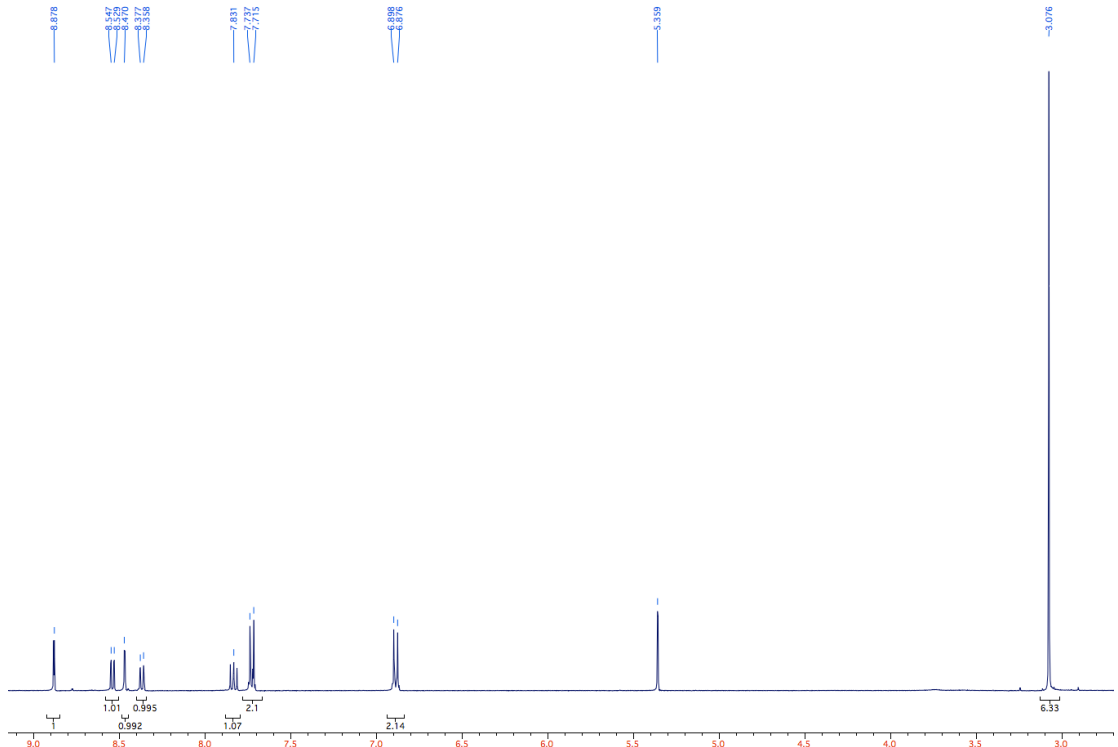


Figure S5: ^1H NMR spectrum of **4** in CD_2Cl_2 .

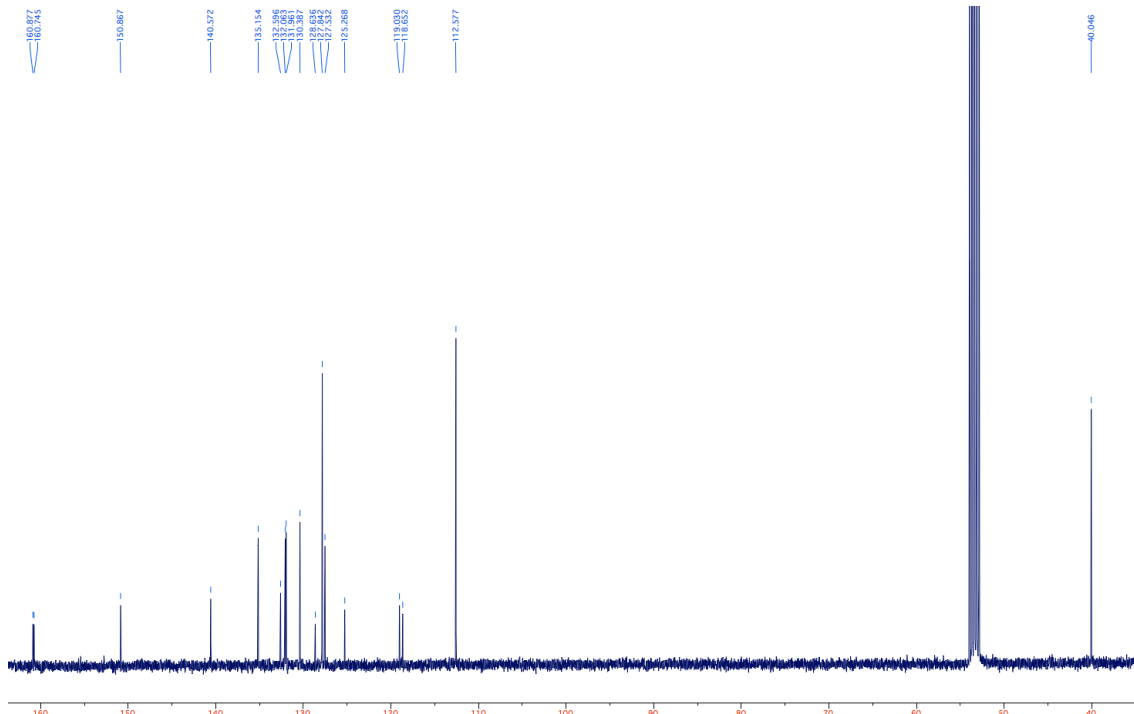


Figure S6: $^{13}\text{C}\{^1\text{H}\}$ NMR spectrum of **4** in CD_2Cl_2 .

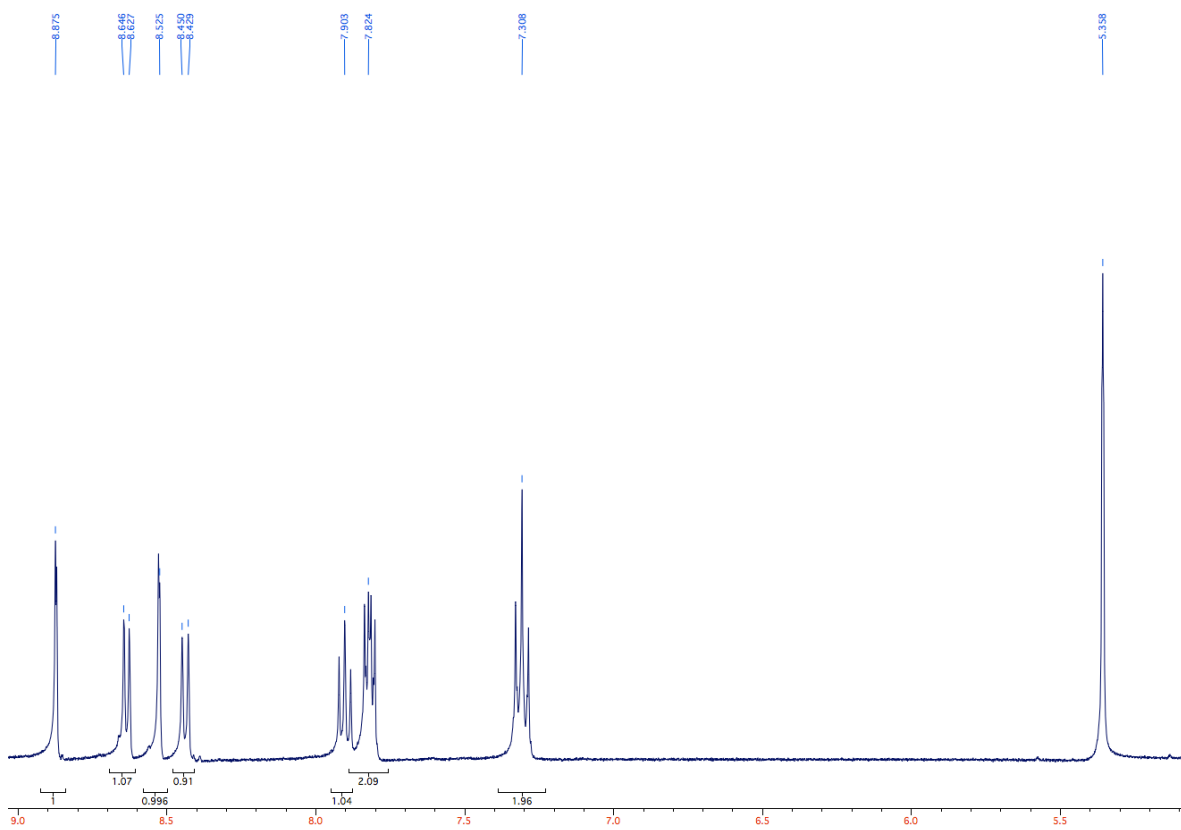


Figure S7: ^1H NMR spectrum of **5** in CD_2Cl_2 .

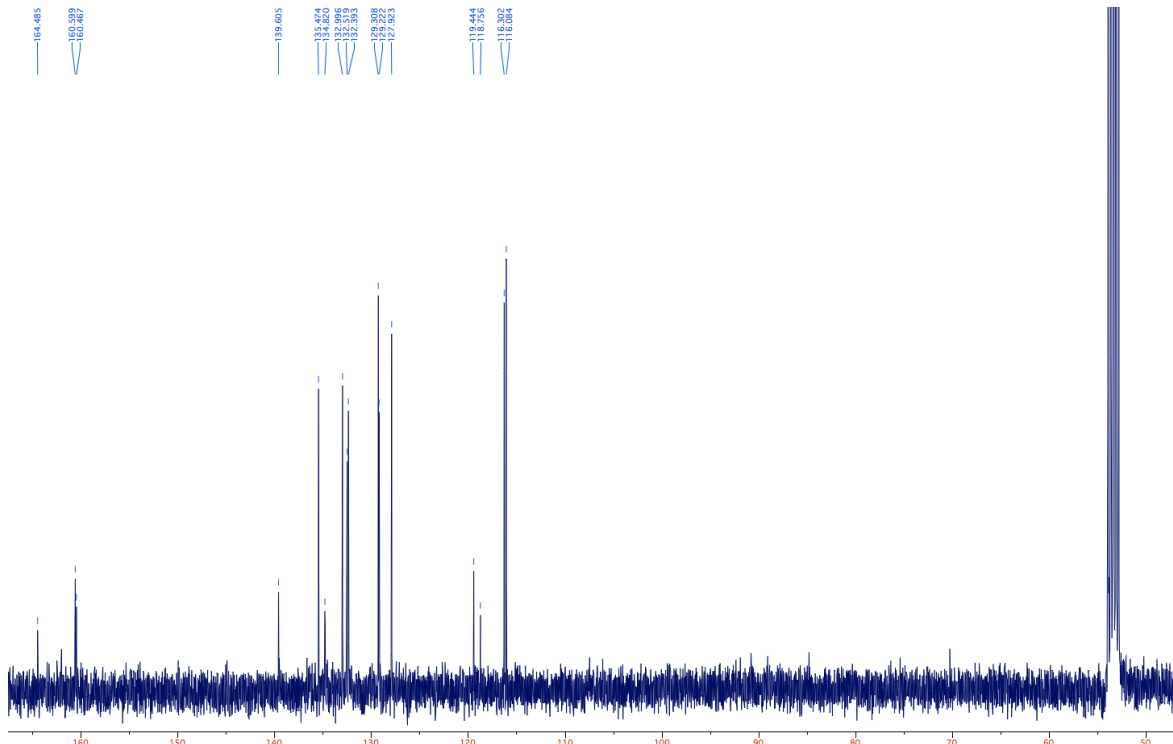


Figure S8: $^{13}\text{C}\{\text{H}\}$ NMR spectrum of **5** in CD_2Cl_2 .

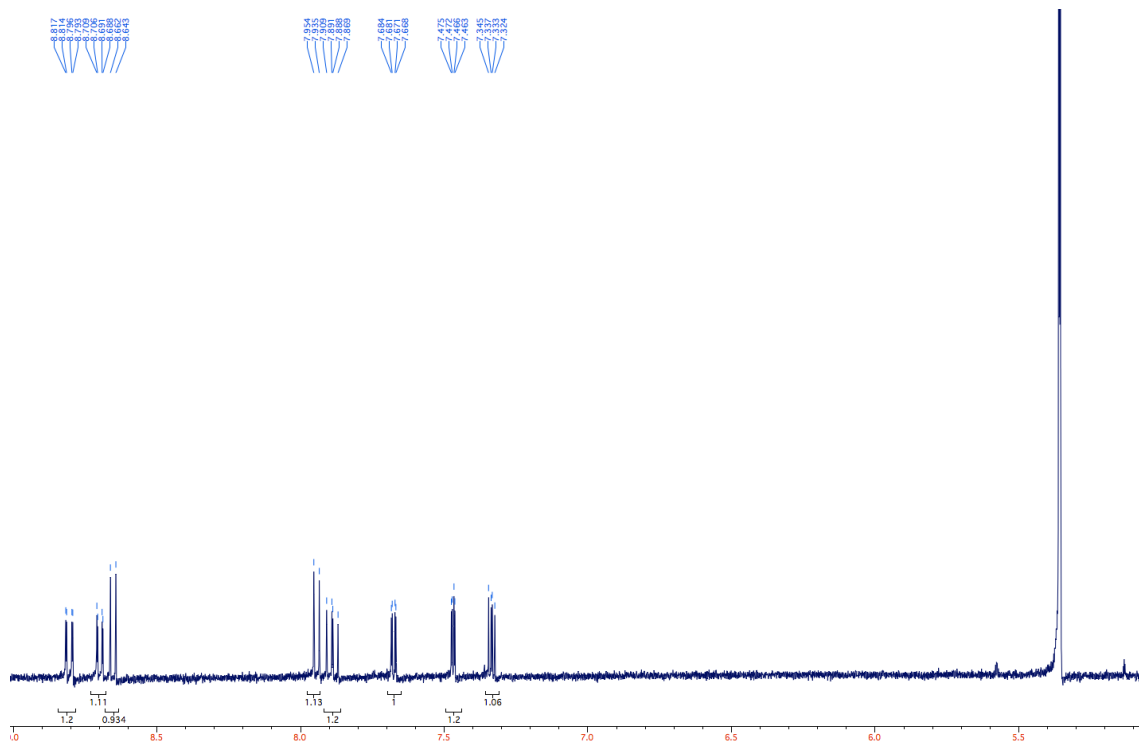


Figure S9: ^1H NMR spectrum of **7** in CD_2Cl_2 .

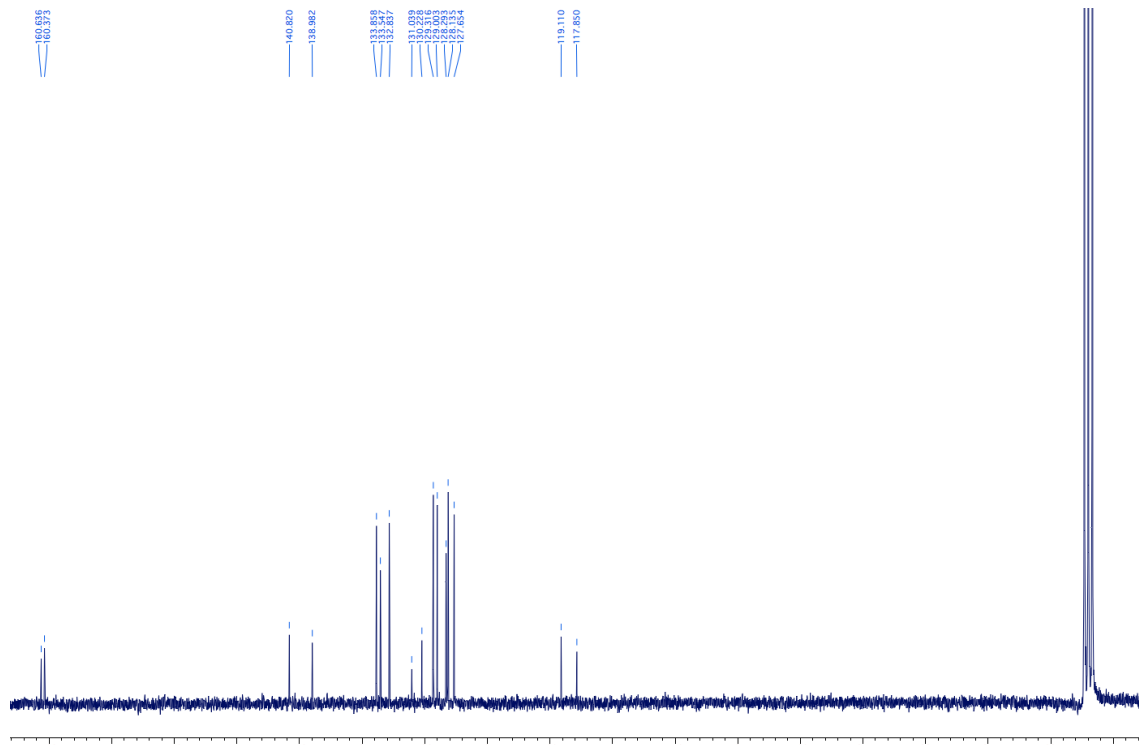


Figure S10: $^{13}\text{C}\{\text{H}\}$ NMR spectrum of **7** in CD_2Cl_2 .

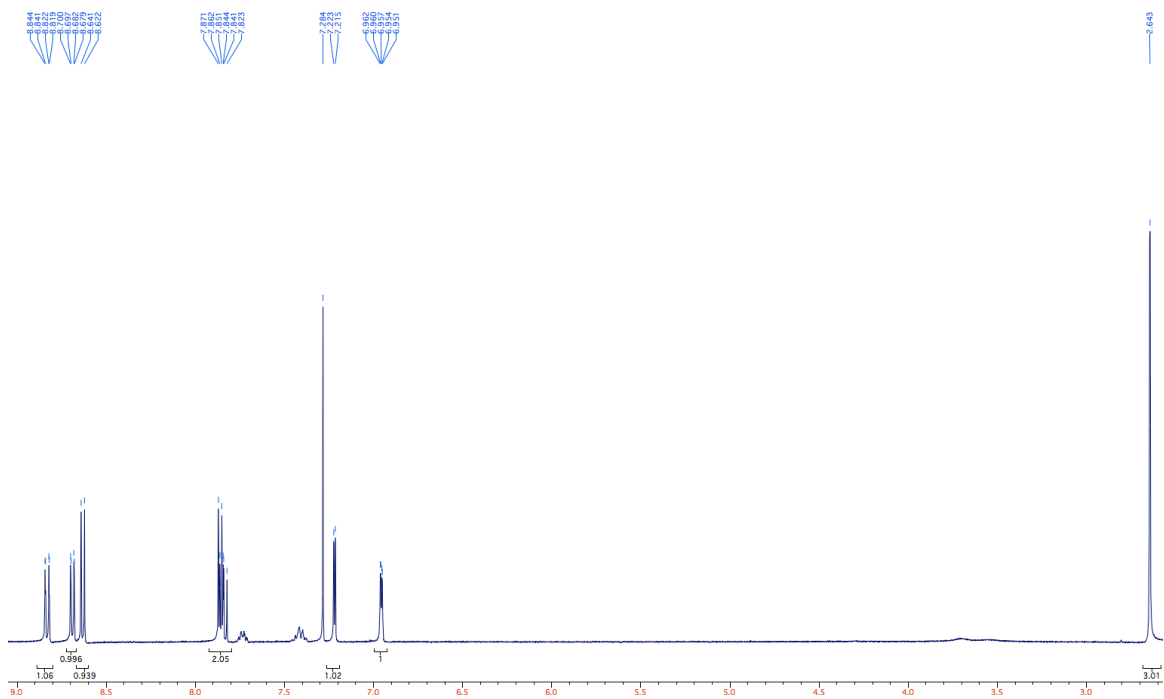


Figure S11: ^1H NMR spectrum of **8** in CDCl_3 . Note: the inseparable impurities at 7.7 ppm and 7.4 ppm can be attributed to dppf from the catalyst used in the Stille coupling toward **8**.

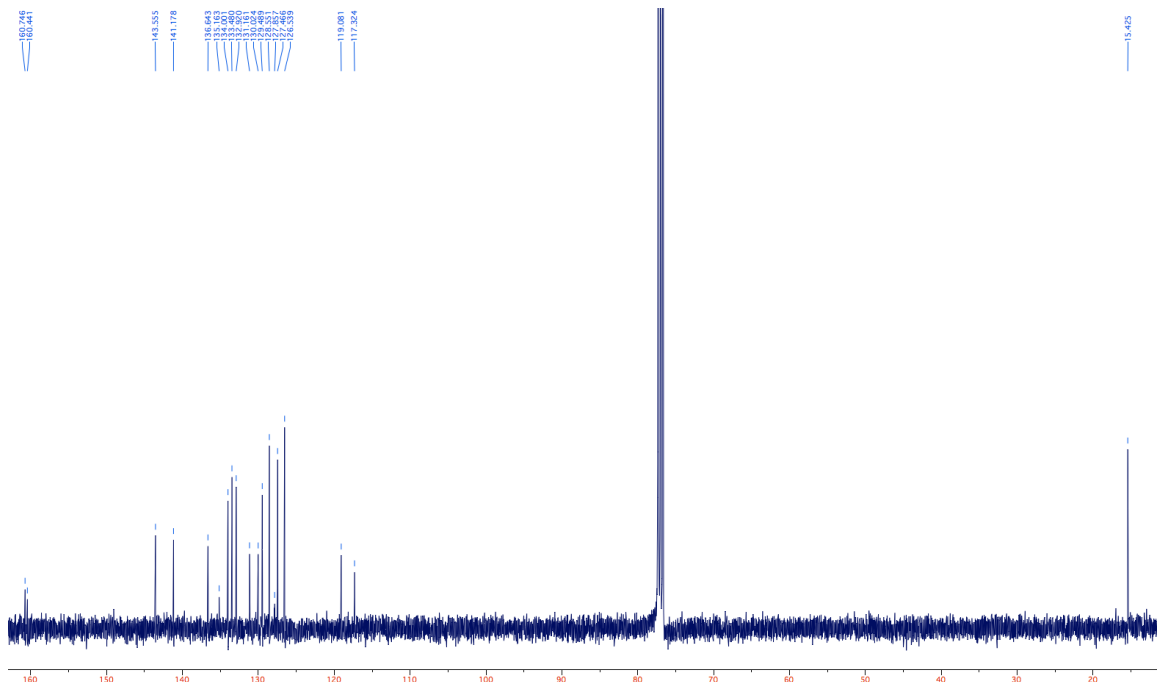


Figure S12: $^{13}\text{C}\{^1\text{H}\}$ NMR spectrum of **8** in CDCl_3 .

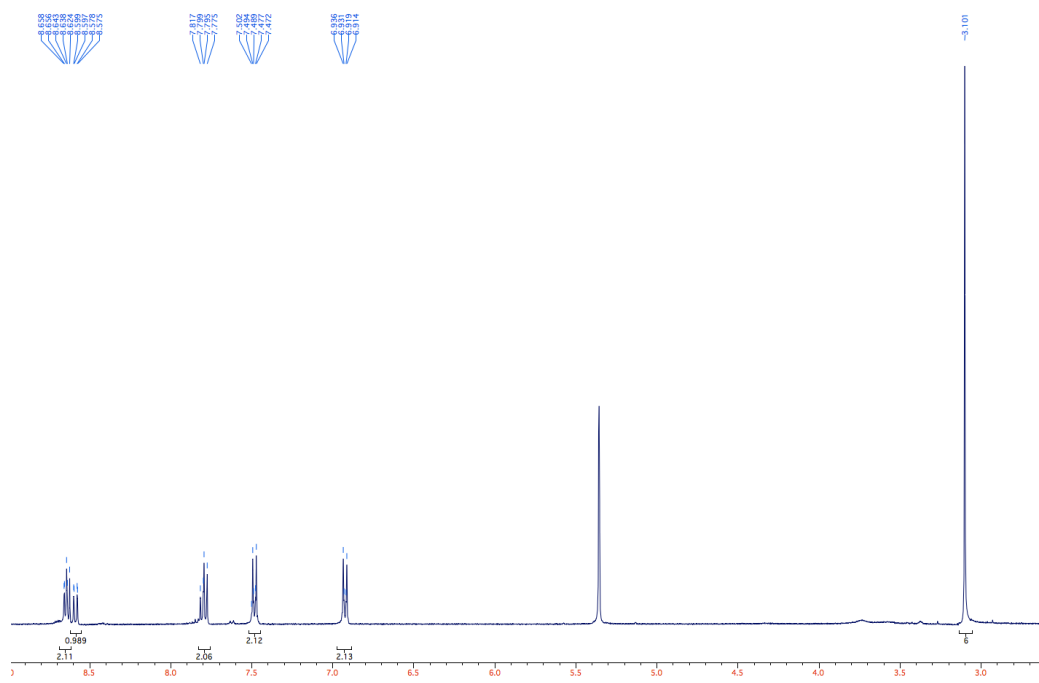


Figure S13: ^1H NMR spectrum of **9** in CD_2Cl_2 .

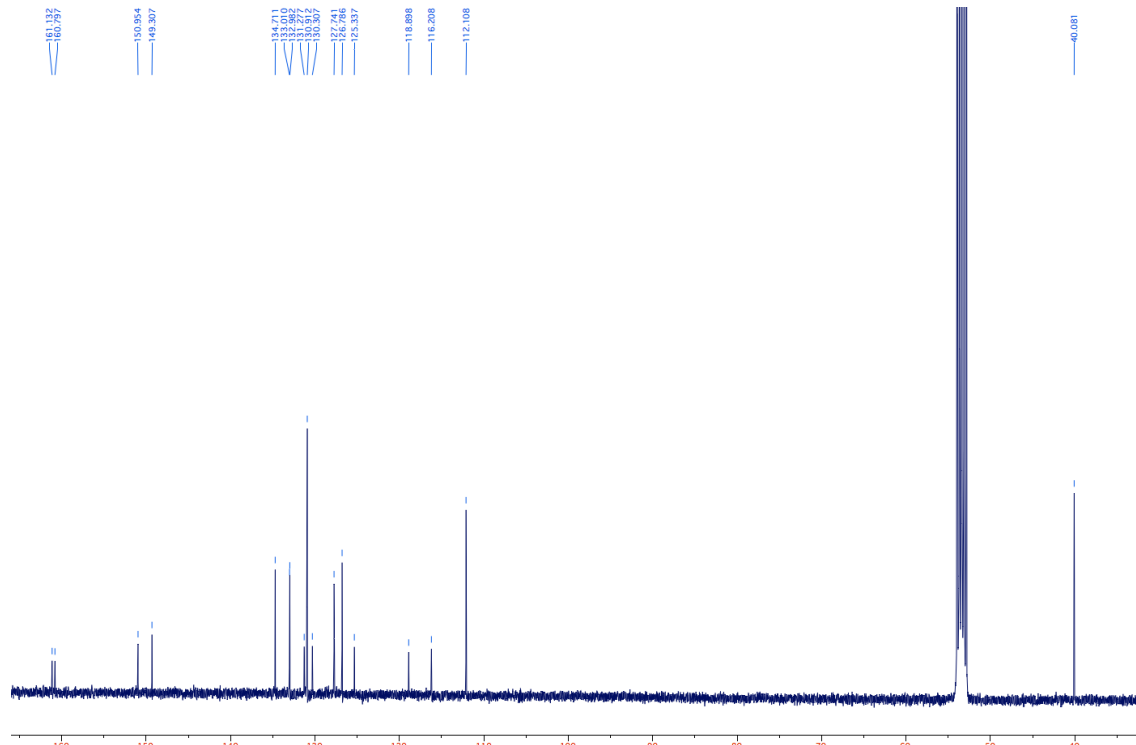


Figure S14: $^{13}\text{C}\{\text{H}\}$ NMR spectrum of **9** in CD_2Cl_2 .

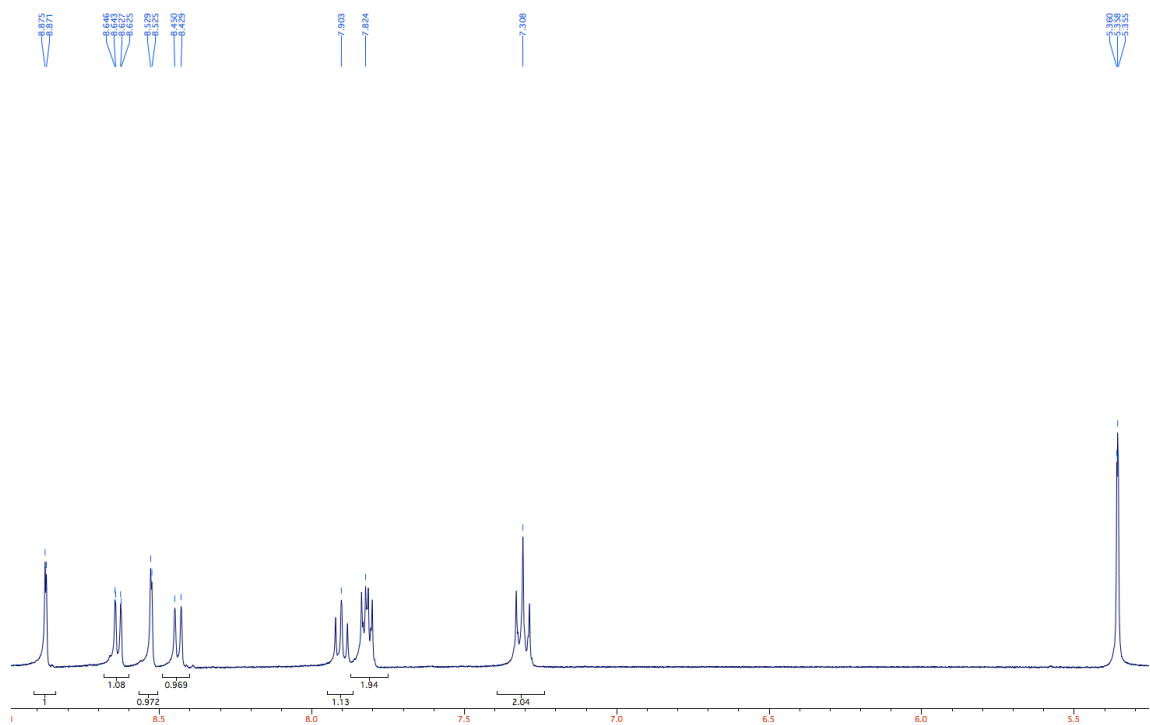


Figure S15: ^1H NMR spectrum of **10** in CD_2Cl_2 .

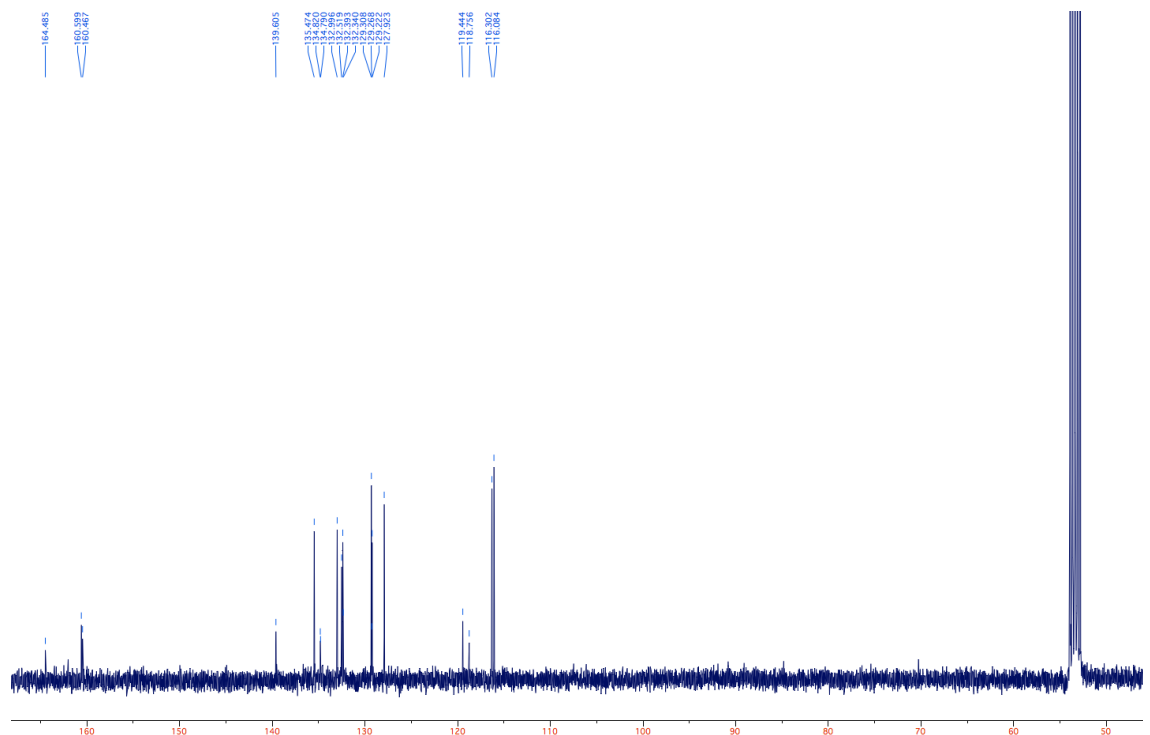


Figure S16: $^{13}\text{C}\{^1\text{H}\}$ NMR spectrum of **10** in CDCl_3 .

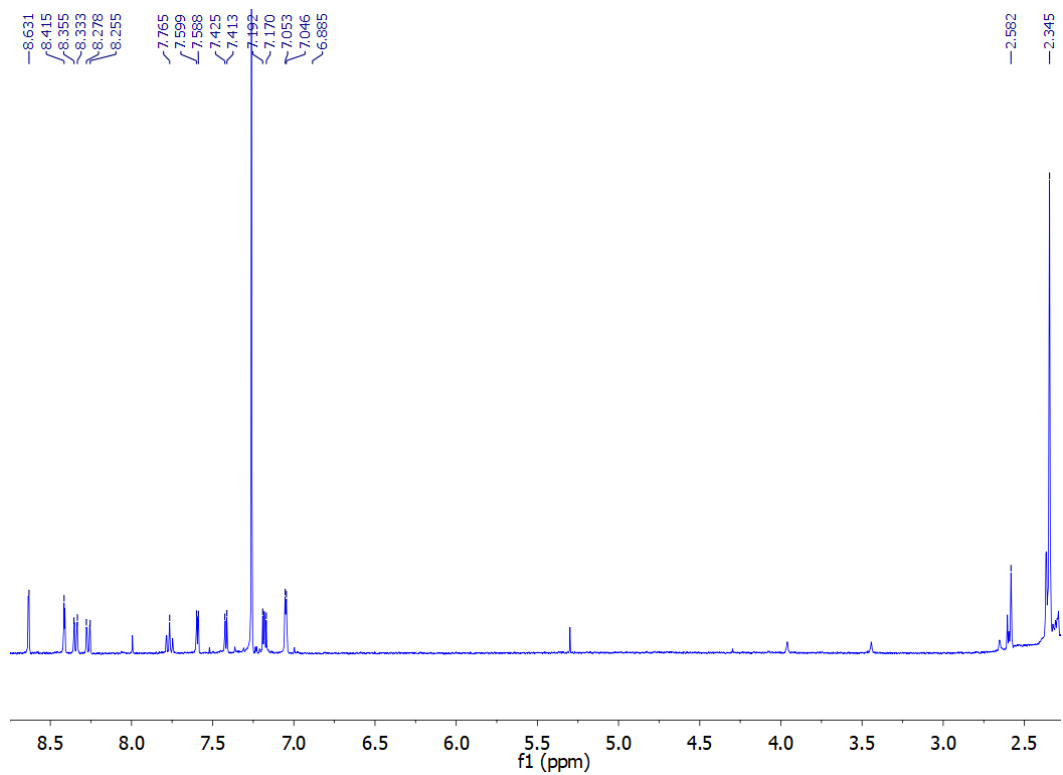


Figure S17: ^1H NMR spectrum of **11** in CDCl_3 .

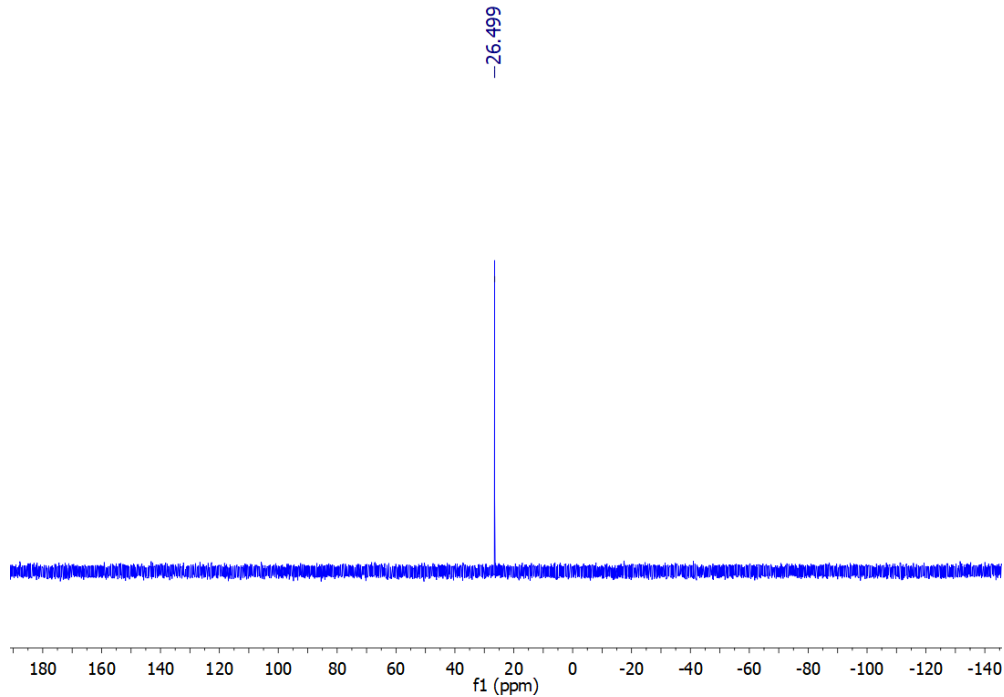


Figure S18: $^{31}\text{P}\{\text{H}\}$ NMR spectrum of **11** in CDCl_3 .

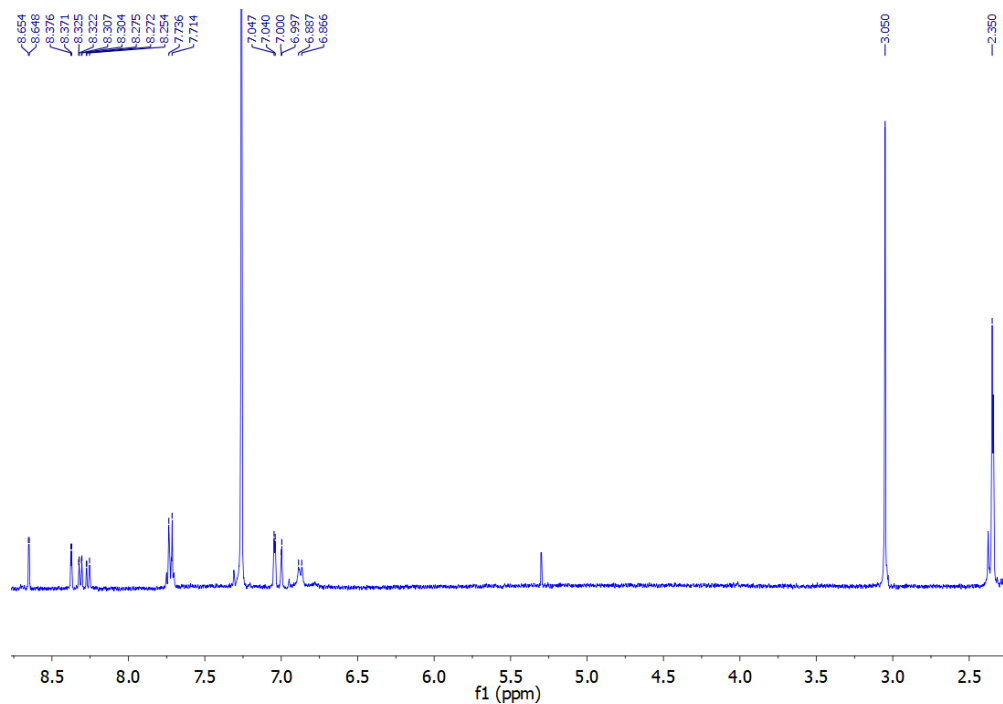


Figure S19: ^1H NMR spectrum of **12** in CDCl_3 .

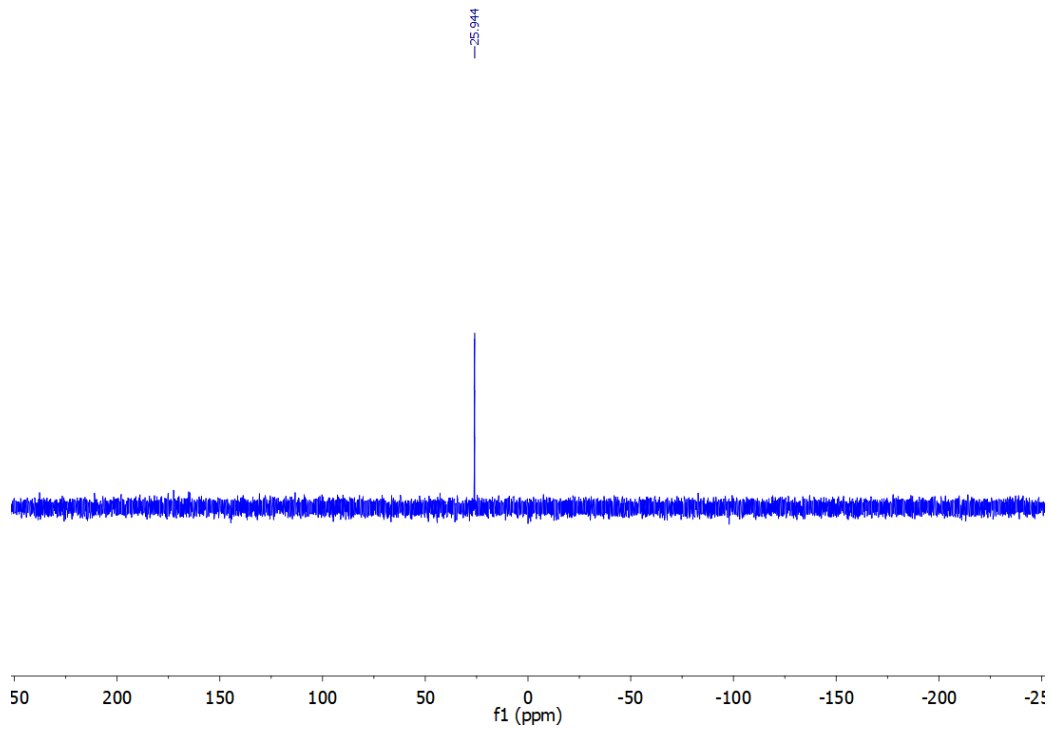


Figure S20: $^{31}\text{P}\{\text{H}\}$ NMR spectrum of **12** in CDCl_3 .

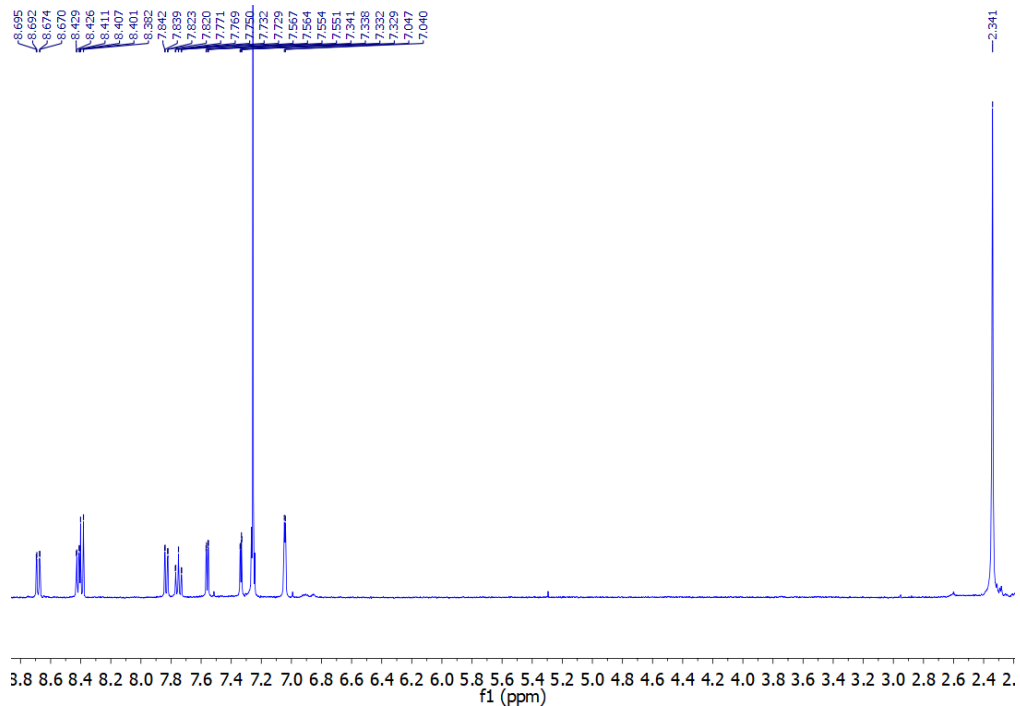


Figure S21: ^1H NMR spectrum of **13** in CDCl_3 .

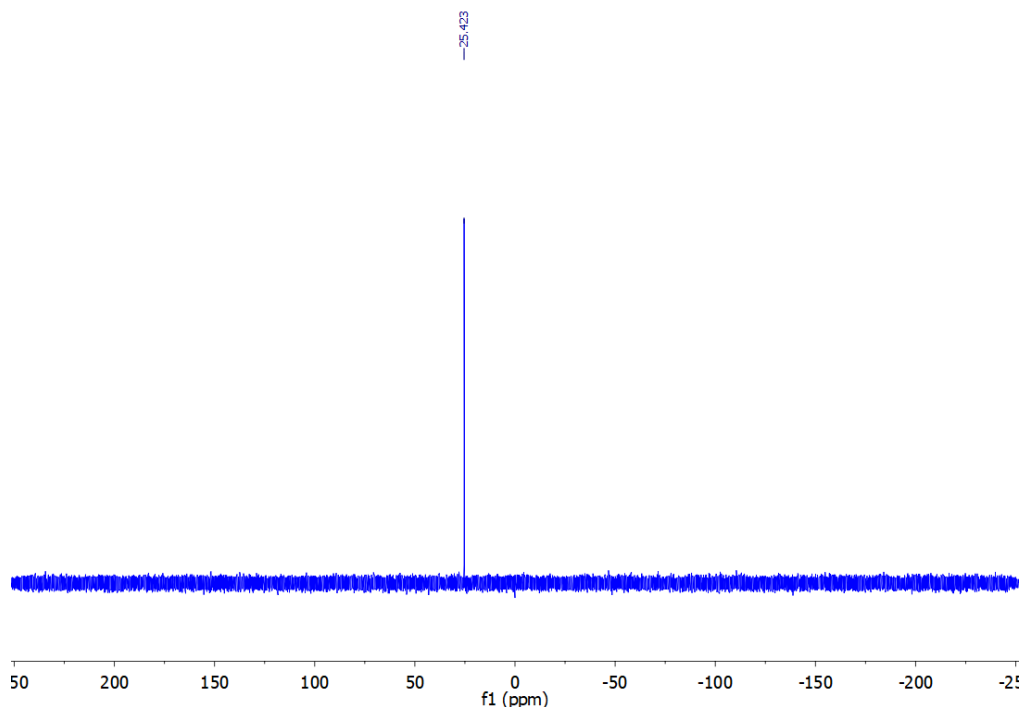


Figure S22: $^{31}\text{P}\{^1\text{H}\}$ NMR spectrum of **13** in CDCl_3 .

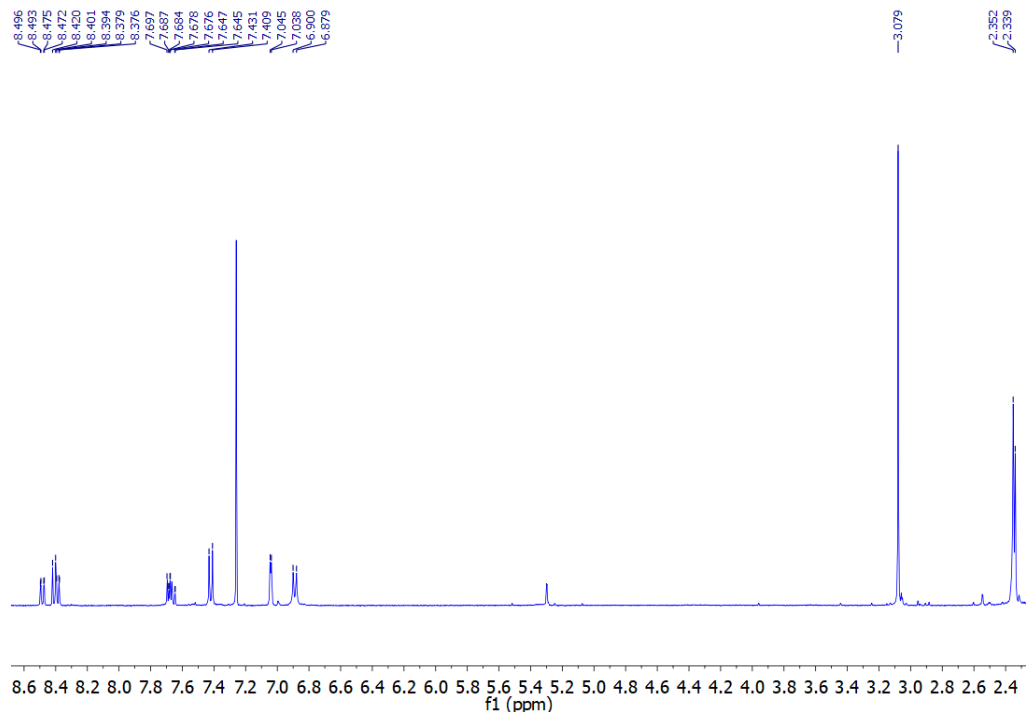


Figure S23: ^1H NMR spectrum of **14** in CDCl_3 .

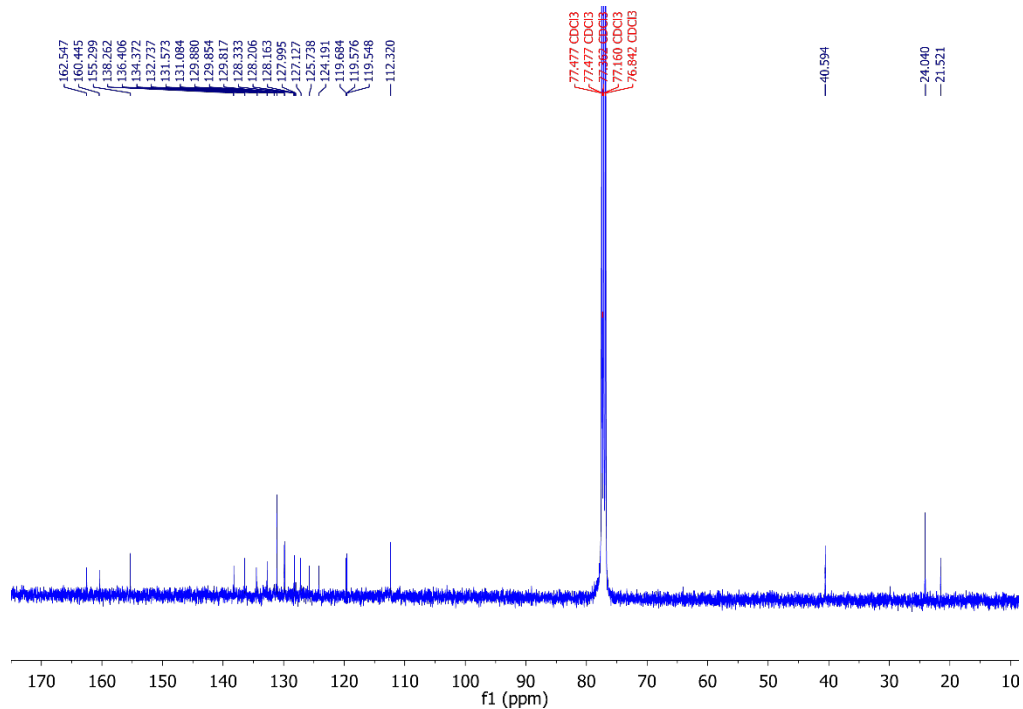


Figure S24: $^{13}\text{C}\{^1\text{H}\}$ NMR spectrum of **14** in CDCl_3 .

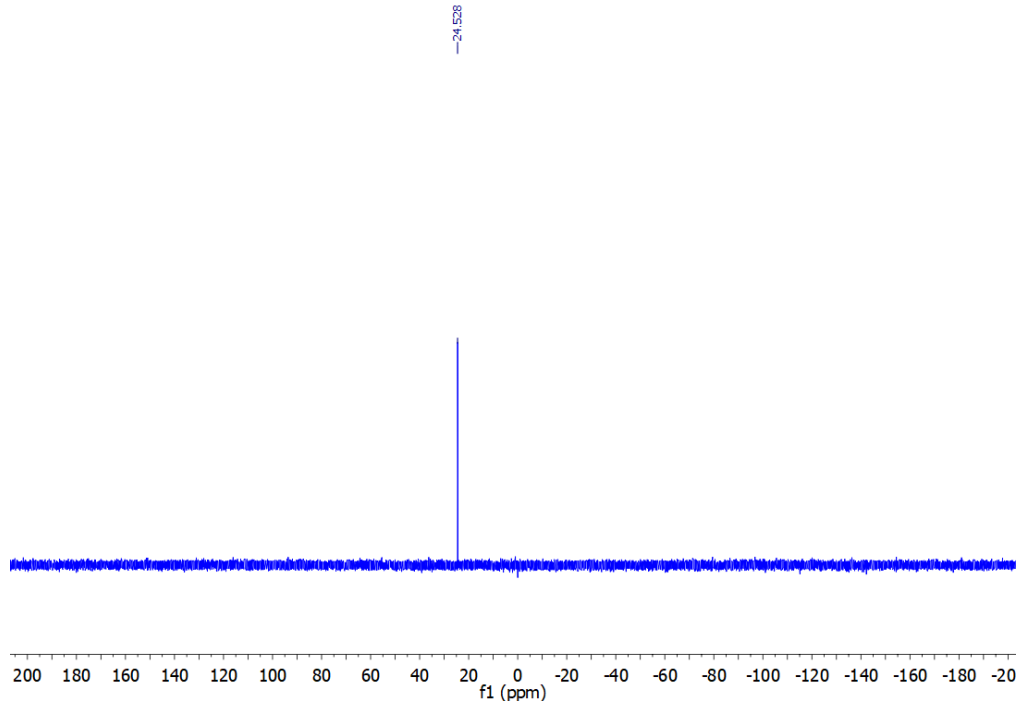


Figure S25: $^{31}\text{P}\{\text{H}\}$ NMR spectrum of **14** in CDCl_3 .

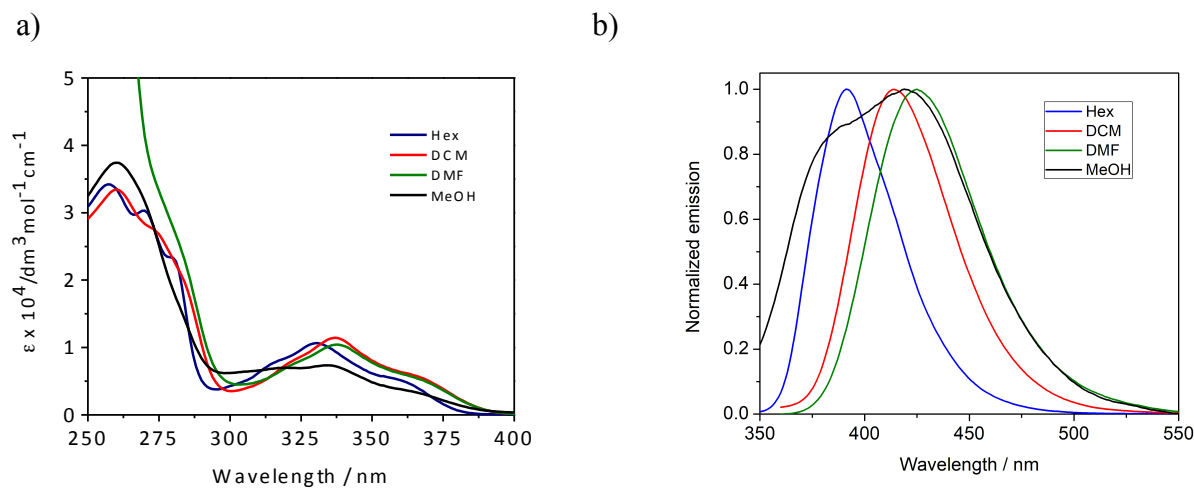


Figure S26: Absorption (a) and normalized emission (b) spectra of **1** in various solvents (5×10^{-5} M).

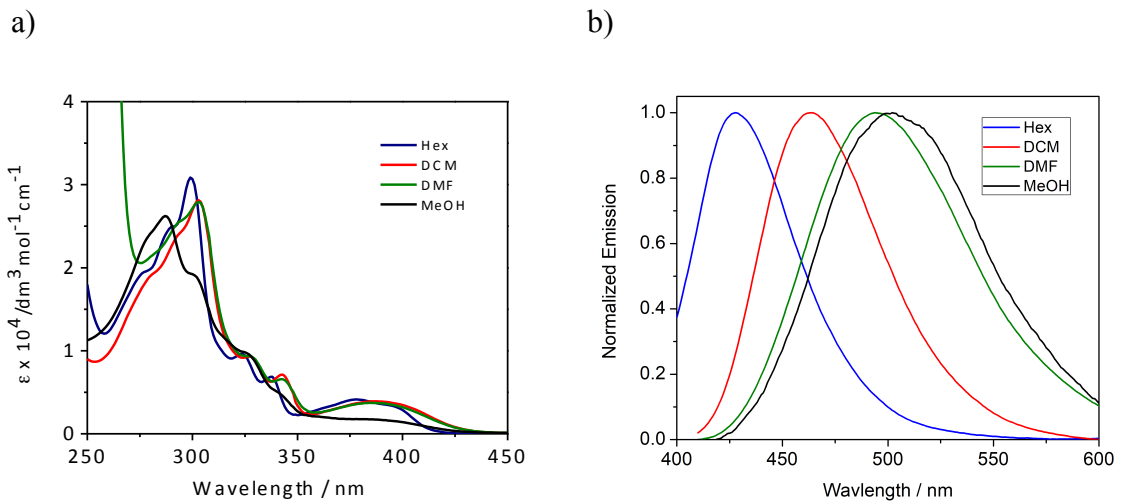


Figure S27: Absorption (a) and normalized emission (b) spectra of **2** in various solvents (5×10^{-5} M).

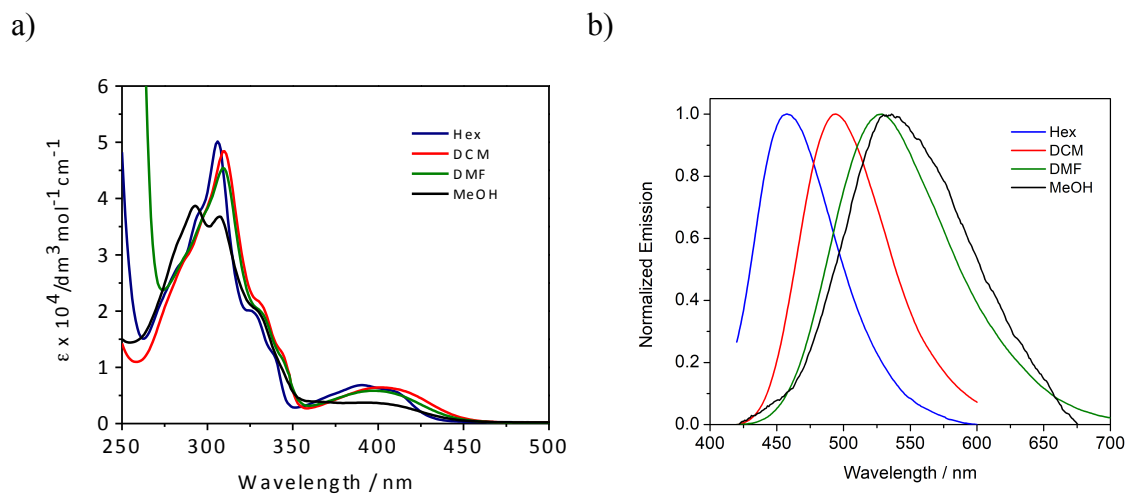


Figure S28: Absorption (a) and normalized emission (b) spectra of **3** in various solvents (5×10^{-5} M).

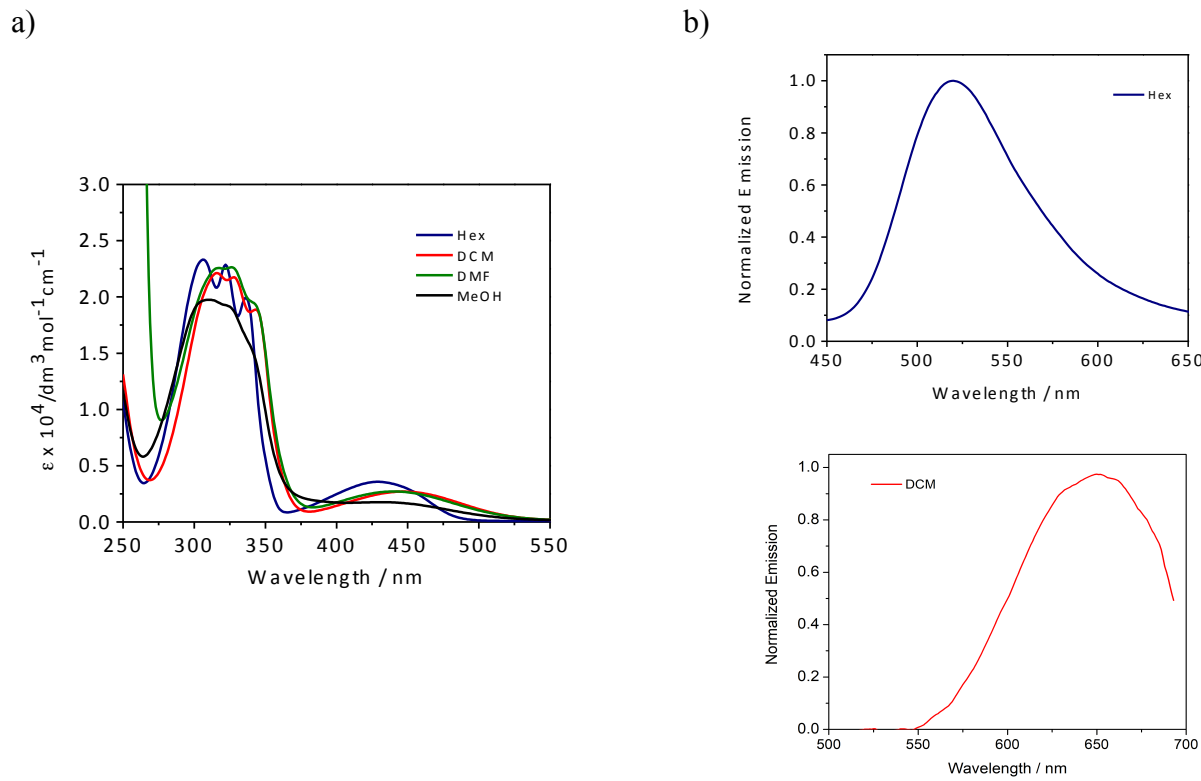


Figure S29: Absorption (a) and normalized emission (b) spectra of **4** in various solvents (5×10^{-5} M).

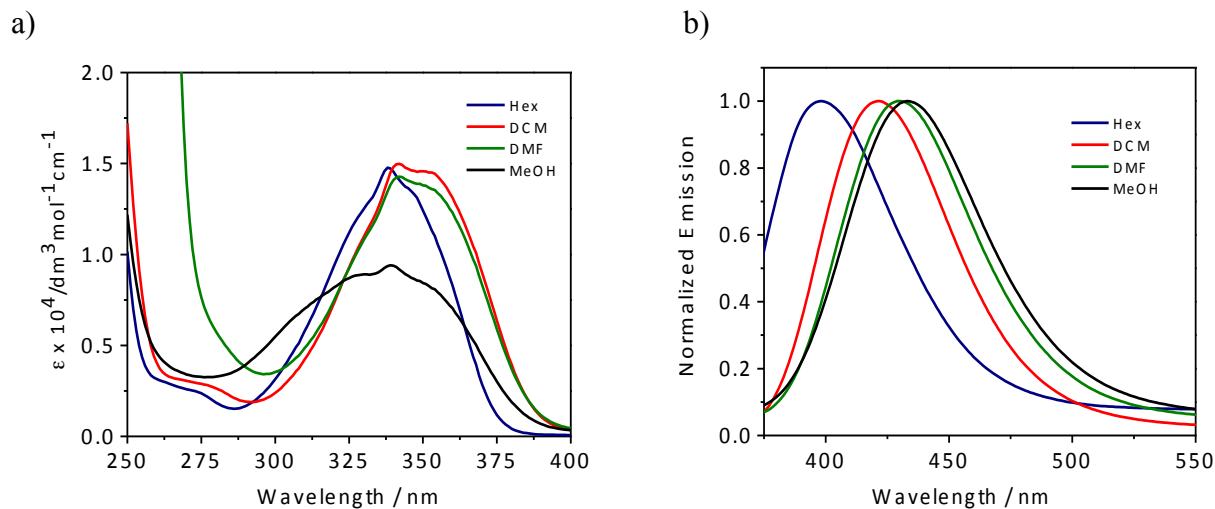


Figure S30: Absorption (a) and normalized emission (b) spectra of **6** in various solvents (5×10^{-5} M).

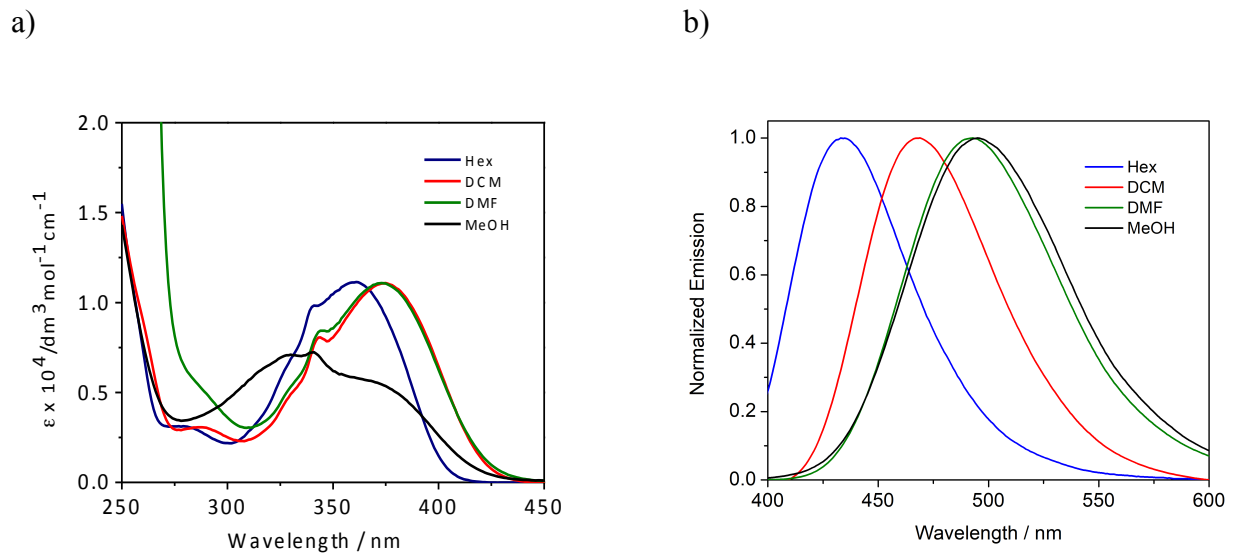


Figure S31: Absorption (a) and normalized emission (b) spectra of **7** in various solvents (5×10^{-5} M).

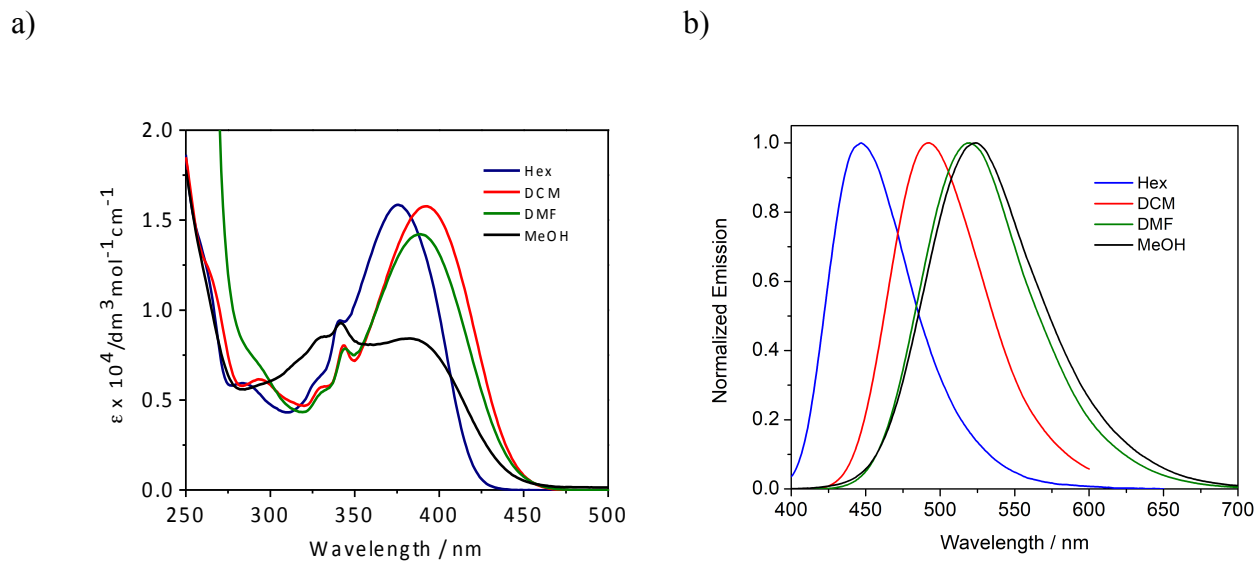


Figure S32: Absorption (a) and normalized emission (b) spectra of **8** in various solvents (5×10^{-5} M).

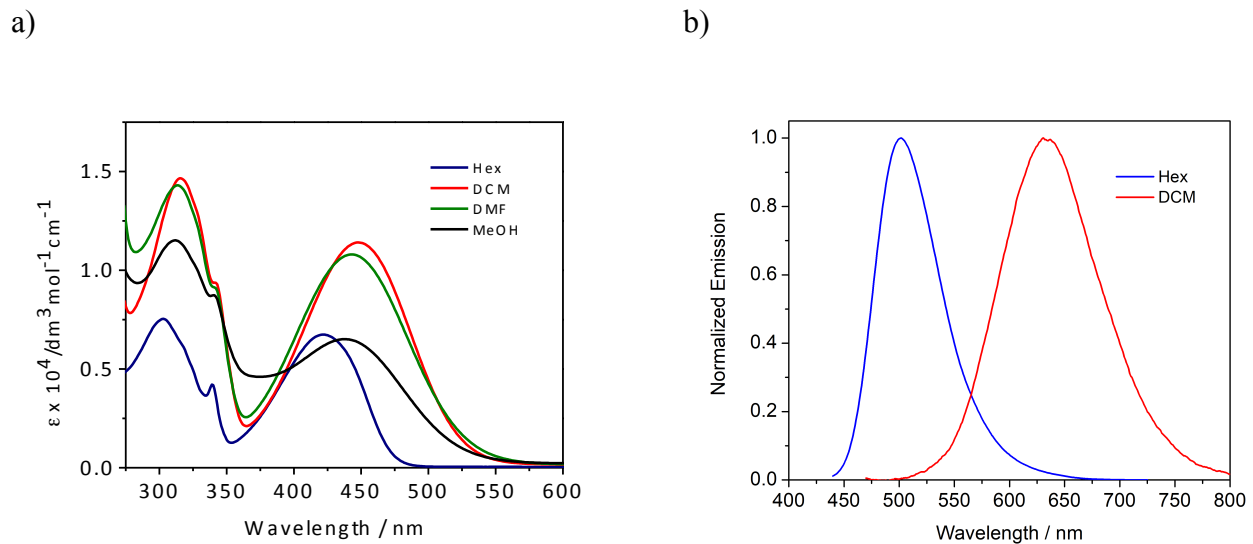


Figure S33: Absorption (a) and normalized emission (b) spectra of **9** in various solvents (5×10^{-5} M).

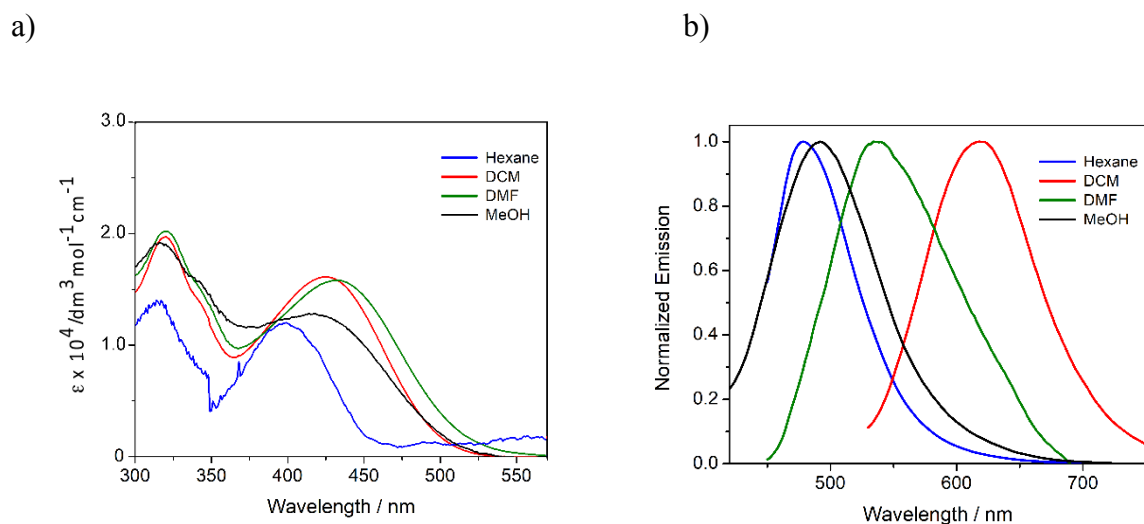


Figure S34: Absorption (a) and normalized emission (b) spectra of **14** in various solvents.

Table S1. Solvatochromism data of compounds **1-4**, **6-9** and **14**.

Compound	Solvent	λ_{abs} [nm]	λ_{em} [nm]
1	Hexane	330	391
	DCM	337	414
	DMF	338	425
	MeOH	333	419
2	Hexane	378	428
	DCM	388	464
	DMF	385	494
	MeOH	360	502
3	Hexane	391	458
	DCM	402	494
	DMF	397	529
	MeOH	370	536
4	Hexane	429	520
	DCM	445	670
	DMF	443	-
	MeOH	430	-
6	Hexane	338	398
	DCM	342	421
	DMF	342	430
	MeOH	339	433
7	Hexane	361	433
	DCM	375	469
	DMF	373	493
	MeOH	341	495
8	Hexane	376	447
	DCM	392	493
	DMF	388	520
	MeOH	382	524
9	Hexane	422	502
	DCM	448	631
	DMF	443	-
	MeOH	438	-
14	Hexane	397	477
	DCM	425	619
	DMF	432	536
	MeOH	420	492

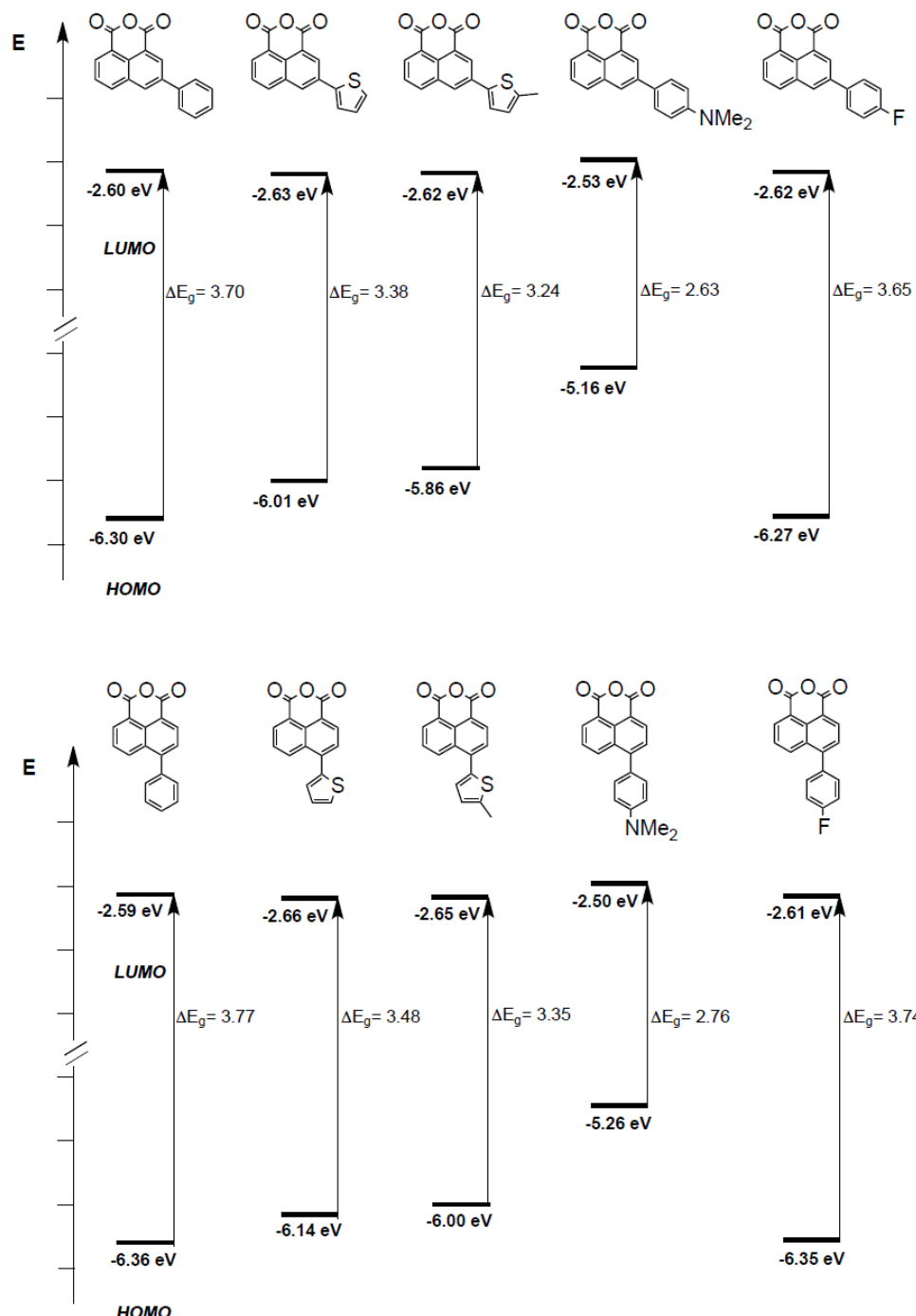


Figure S35. HOMO and LUMO levels (B3LYP/6-31G(d)) of compounds **1-10**. $\Delta E_g = -(E_{\text{LUMO}} - E_{\text{HOMO}})$.

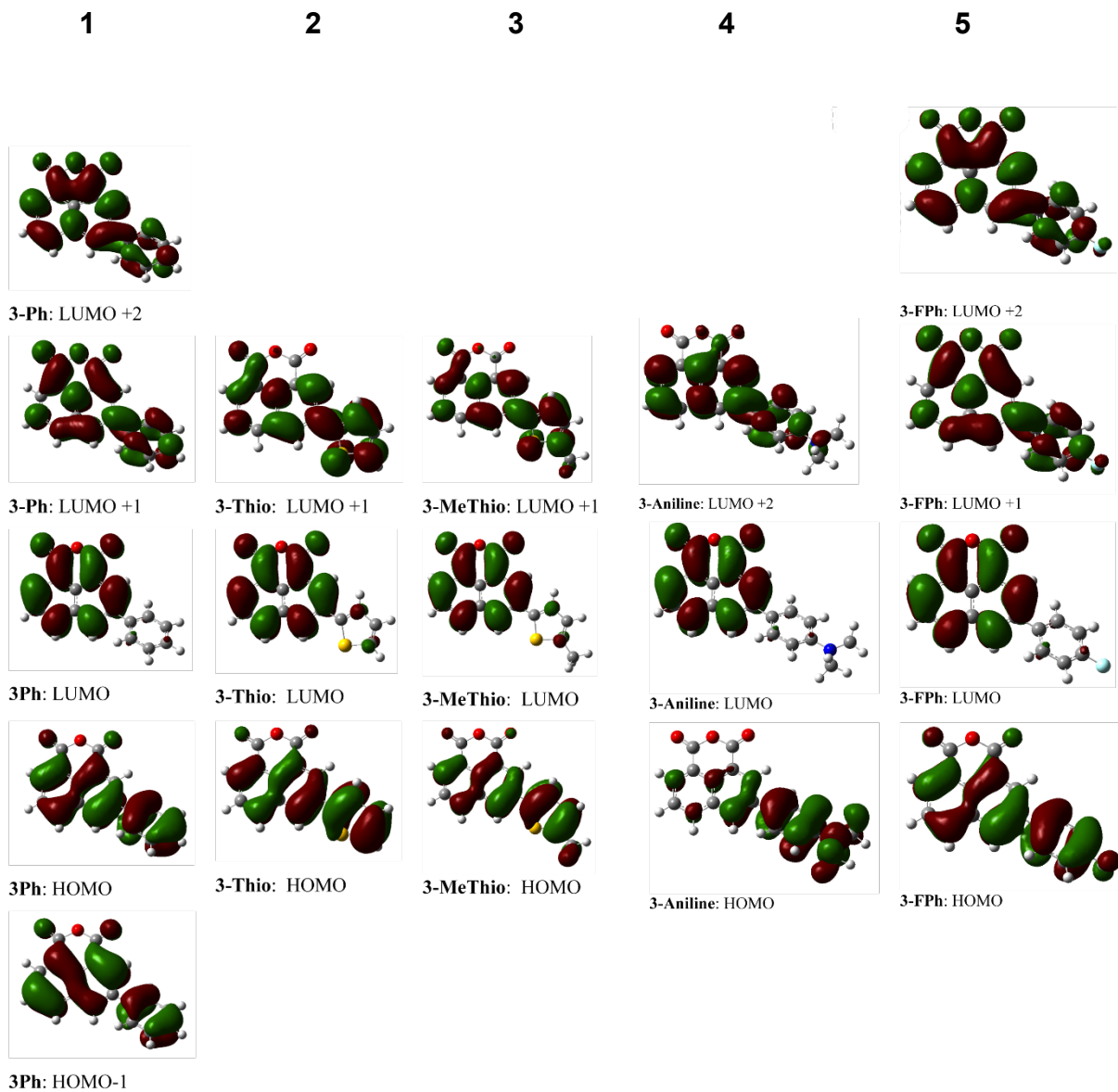


Figure S36: Frontier Molecular Orbitals for compounds **1-5**.

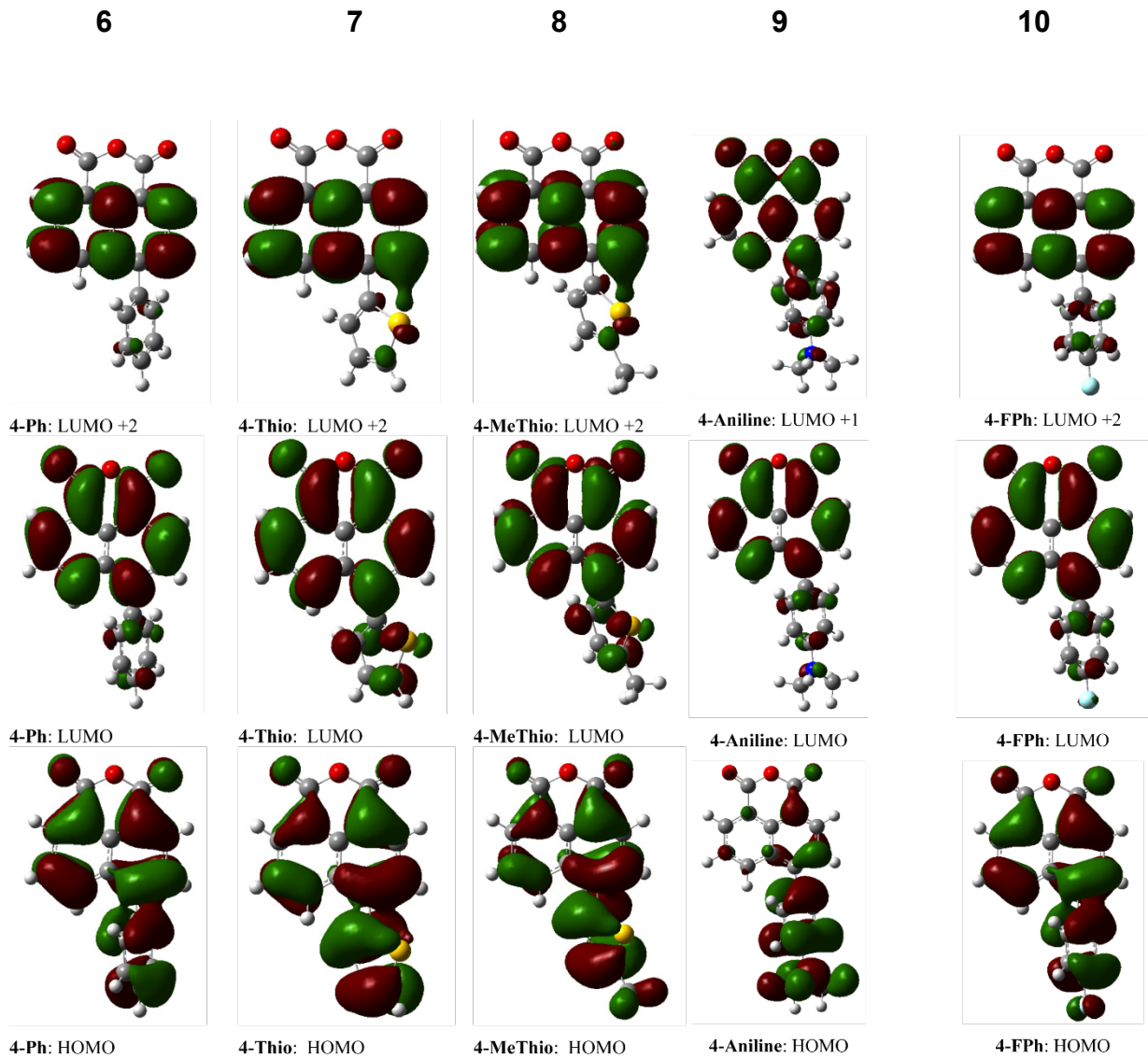


Figure S37: Frontier Molecular Orbitals for compounds **6-10**.

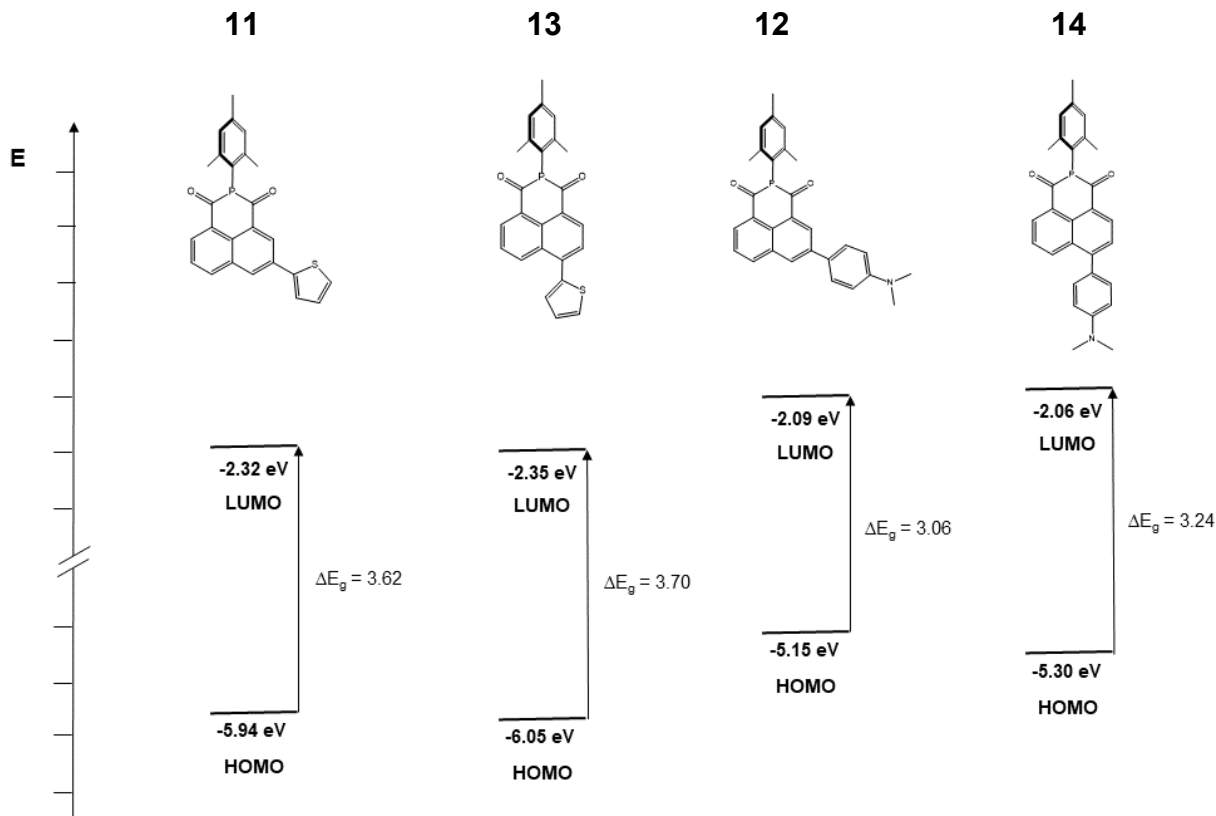


Figure S38. HOMO and LUMO levels (B3LYP/6-31G(d)) of compounds **11-14**. $\Delta E_g = -(E_{\text{LUMO}} - E_{\text{HOMO}})$.

Table S2. HOMO/LUMO energy gaps calculated and generated from the UV-vis spectra.

	ΔE_g (eV) ^a	λ_{abs} (eV)
1	3.70	3.68
2	3.38	3.19
3	3.24	3.09
4	2.63	2.78
5	3.65	3.68
6	3.77	3.63
7	3.48	3.31
8	3.35	3.15
9	2.76	2.77
10	3.74	3.64
11	3.62	3.24
12	3.70	3.03
13	3.06	3.26
14	3.24	2.92

^a Calculated with Gaussian 09; B3LYP/6-31G(d) level of theory; $\Delta E_g = -(E_{\text{LUMO}} - E_{\text{HOMO}})$

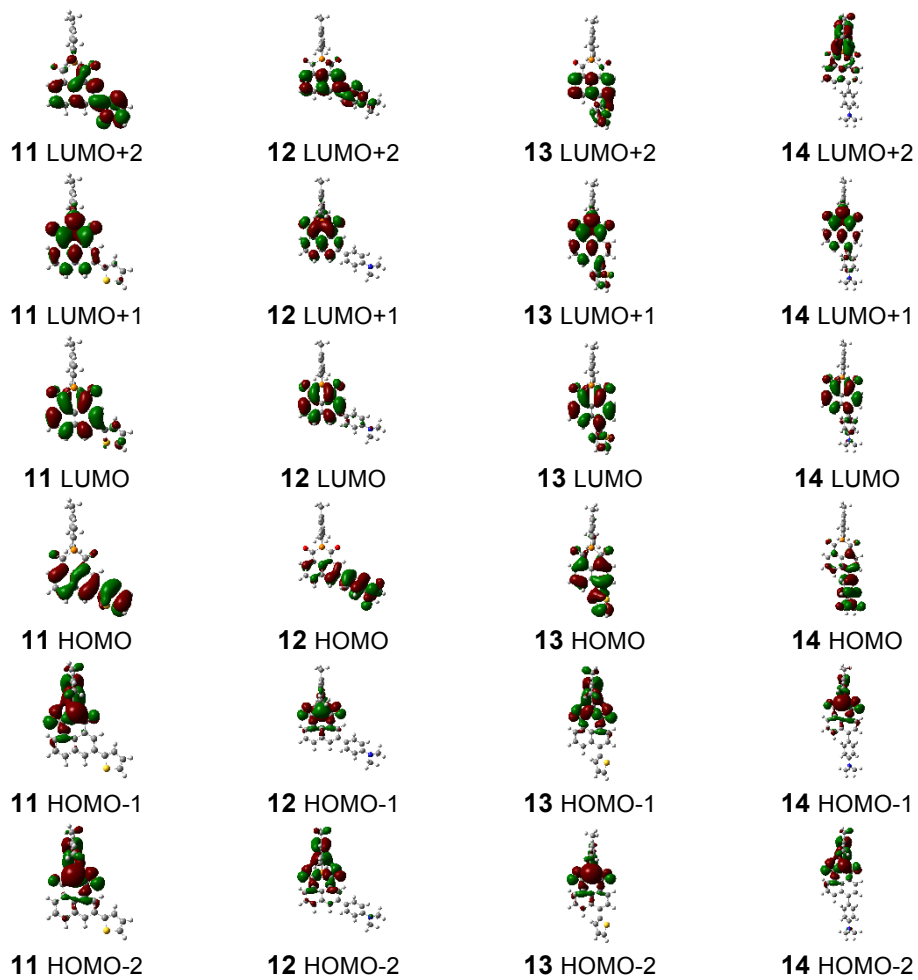


Figure S39: Frontier Molecular Orbitals for compounds **11-14**.

Table S3. TD-DFT calculated transition data (B3LYP/6-31G(d)) in dichloromethane.

Compound	Transitions	λ [nm]	f^b
1	HOMO – LUMO (85%) ^a	378.01	0.0981
	HOMO-1 – LUMO (79%)	327.48	0.1793
	HOMO – LUMO+2 (43%)	262.72	0.8248
	HOMO – LUMO+1 (18%)		
2	HOMO – LUMO (88%)	421	0.0933
	HOMO – LUMO+1 (73%)	298.48	0.8023
3	HOMO – LUMO (89%)	440.48	0.0934
	HOMO – LUMO+1 (75%)	307.6	0.9169
4	HOMO – LUMO (95%)	557.95	0.0679
	HOMO – LUMO+2 (79%)	331.04	0.5946
5	HOMO – LUMO (87%)	384.33	0.0915
	HOMO – LUMO+2 (52%)	264.75	0.9246
	HOMO – LUMO+1 (18%)		
6	HOMO – LUMO (85%)	369.1	0.3777
	HOMO – LUMO+2 (62%)	245.35	0.2511
7	HOMO – LUMO (87%)	405.61	0.3814
	HOMO – LUMO+2 (72%)	260.33	0.2164
8	HOMO – LUMO (88%)	423.16	0.3963
	HOMO – LUMO+2 (72%)	267.62	0.1829
9	HOMO – LUMO (93%)	525.48	0.2822
	HOMO – LUMO+1 (81%)	335.66	0.3501
10	HOMO – LUMO (86%)	374.12	0.3661
	HOMO – LUMO+2 (68%)	247.38	0.2585
11	HOMO – LUMO (88%)	400.15	0.0696
	HOMO-2 – LUMO (7%)		
	HOMO-4 – LUMO (60%)	331.9	0.1574
	HOMO-1 – LUMO (16%)		
	HOMO-6 – LUMO (80%)	303.37	0.1762
	HOMO – LUMO+2 (63%)	297.13	0.7867
	HOMO-6 – LUMO (17%)		

	HOMO-7 – LUMO (55%) HOMO-4 – LUMO+2 (10%)	277.01	0.1221
12	HOMO – LUMO (96%)	403.69	0.1028
	HOMO – LUMO+1 (92%)	289.03	0.1892
	HOMO – LUMO+2 (67%)	277.83	0.3128
	HOMO-3 – LUMO (88%)	275.09	0.4731
13	HOMO – LUMO (66%)	393.1	0.3407
	HOMO-1 – LUMO (19%)		
	HOMO-1 – LUMO (52%)	386.47	0.1344
	HOMO – LUMO (26%)		
	HOMO-4 – LUMO+1 (55%)	271.22	0.0500
	HOMO-5 – LUMO+1 (17%)		
	HOMO – LUMO+3 (31%)	256.31	0.2431
	HOMO-2 – LUMO+2 (18%)		
	HOMO-1 – LUMO+2 (11%)		
	HOMO – LUMO+4 (12%)		
	HOMO-8 – LUMO+1 (31%)	239.06	0.3562
	HOMO-9 – LUMO (18%)		
14	HOMO-1 – LUMO+2 (12%)		
	HOMO – LUMO (99%)	493.21	0.3256
	HOMO – LUMO+1 (96%)	396.23	0.1073
	HOMO-1 – LUMO (93%)	340.11	0.3309
	HOMO – LUMO+7 (77%)	244.44	0.5819

^a The coefficient percentages of the orbitals involved in the transitions.

f= oscillator strength

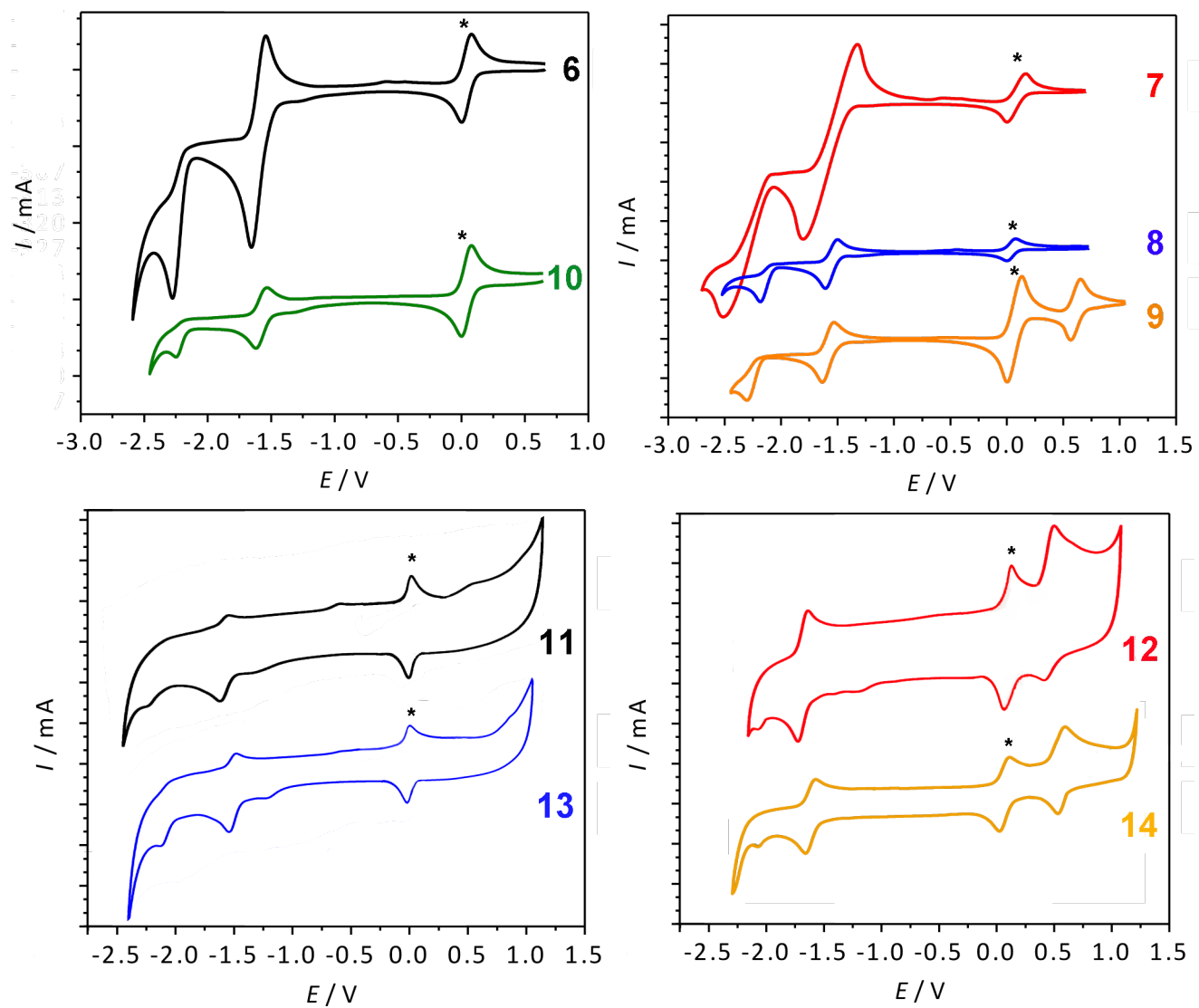


Figure S40. Cyclic voltammograms of compounds **6-14** in CH_2Cl_2 solution containing 0.1 M tetrabutylammonium hexafluorophosphate as the supporting electrolyte. Scan rate = 100 mV/s. Ferrocene (*) was added as an internal standard and referenced to 0 V.